RSC Advances

REVIEW

View Article Online
View Journal | View Issue

Cite this: *RSC Adv.*, 2015, **5**, 22759

Recent advances in methanation catalysts for the production of synthetic natural gas

Jiajian Gao,[ab] Qing Liu,[a] Fangna Gu,[a] Bin Liu,*[b] Ziyi Zhong[c] and Fabing Su*[a]

Received 10th December 2014
Accepted 18th February 2015

DOI: 10.1039/c4ra16114a

www.rsc.org/advances

Methanation of coal- or biomass-derived carbon oxides for production of synthetic natural gas (SNG) is gaining considerable interest due to energy issues and the opportunity of reducing greenhouse gases by carbon dioxide conversion. The key component of the methanation process is the catalyst design. Ideally, the catalyst should show high activity at low temperatures (200–300 °C) and high stability at high temperatures (600–700 °C). In the past decades, various methanation catalysts have been investigated, among which transition metals including Ni, Fe, Co, Ru, Mo, *etc.* dispersed on metal oxide supports such as Al_2O_3, SiO_2, TiO_2, ZrO_2, CeO_2 *etc.* have received great attention due to their relatively high catalytic activity and selectivity. Furthermore, over the past few years, great efforts have been made both in methanation catalysts development and reaction mechanism investigation. Here we provide a comprehensive review to these most advancements, covering the reaction thermodynamics, mechanism and kinetics, the effects of catalyst active components, supports, promoters and preparation methods, hoping to outline the pathways for the future methanation catalysts design and development for SNG production.

1. Introduction

Among different forms of fossil fuels, natural gas that consists primarily of methane is ideal, owing to its ready availability, high energy density and conversion efficiency, and smoke- and slag-free composition.[1] Additionally, natural gas can be transported efficiently at low cost using the existing natural gas pipelines and wide distribution network. In recent years, due to the rise of the natural gas price, the wish for less dependency on natural gas import, and replacement of oil products, synthetic or substitute natural gas (SNG) production from renewable biomass,[2] coke oven gas (COG)[3] or syngas from coal or wood[4] is attracting increasing attention in some countries. Meanwhile, the actively investigated hydrogen production by photocatalytic or electrocatalytic water splitting powered by renewable energies (*e.g.*, solar or wind) is regarded as future sources of hydrogen for carbon dioxide hydrogenation. Hence, the SNG production *via* carbon dioxide methanation process can not only produce fuels and chemicals, but also reduce carbon dioxide emission significantly to the atmosphere.[5–9] Other applications of carbon monoxide methanation include removal of trace carbon monoxide present in H_2-rich gases to produce high purity hydrogen for chemical industry such as NH_3 synthesis and for fuel cells.

The two key reactions of SNG production process are expressed as: $CO + 3H_2 \rightarrow CH_4 + H_2O$, $CO_2 + 4H_2 \rightarrow CH_4 + 2H_2O$. Although the methanation reactions are thermodynamically favorable, catalyst is necessary to obtain an appropriate rate. It should be noted that methanation catalysts for the production of SNG deal with carbon monoxide and/or carbon dioxide at relatively high concentrations, making things quite different as compared with trace carbon monoxide (~1 vol%) removal in hydrogen stream. In the earliest work by Sabatier and Senderens in 1902,[10] nickel was found to be very active for methanation reaction. During the oil crisis in 1970s, the methanation catalysts and reactions were subjected to intensive investigations again because of the interest in producing SNG from naphtha and coal. In particular, Vannice conducted a systemic research on the catalytic synthesis of hydrocarbons from H_2/CO mixtures over group VIII metals (Fe, Co, Ni, Ru, Rh, Pd, Ir, Pt).[11–15] Meanwhile, Mills and Steffgen[16] summarized and reviewed the catalytic methanation of carbon monoxide and carbon dioxide. However, these previous works focus on methanation at relatively low temperatures (about 200–400 °C) which are not optimum for energy recovery.[17,18] Modern SNG processes dealing with high concentrations of carbon monoxide and/or carbon dioxide would result in large temperature increase (hot spots can reach 600–700 °C).[18] It was reported that the methanation catalyst MCR-2X from Haldor Topsøe could be operated at high temperatures with high reaction rates to

[a]*State Key Laboratory of Multiphase Complex Systems, Institute of Process Engineering, Chinese Academy of Sciences, Beijing, China, 100190. E-mail: fbsu@ipe.ac.cn; Fax: +86-10-82544851; Tel: +86-10-82544850*

[b]*School of Chemical and Biomedical Engineering, Nanyang Technological University, 62 Nanyang Drive, Singapore, 637459. E-mail: liubin@ntu.edu.sg; Fax: +65-67947553; Tel: +65-65137971*

[c]*Institute of Chemical Engineering and Sciences, A*star, 1 Pesek Road, Jurong Island, Singapore 627833, Singapore*

produce high-quality steam thus making the process more energy efficient.[18] However, the high operating temperature would accelerate the sintering and coking of the catalyst. In short, the methanation catalysts should be stable at high temperatures and also be active at low temperatures to ignite the reaction in SNG production process.

Over the past ten years, methanation catalysts for the production of SNG have been investigated intensively again and some related reviews have been published, among which, Schildhauer and co-workers[19] did a comprehensive technology review for SNG production from coal and dry biomass in the period from 1950 to 2009. Recently, Wang *et al.*[20] summarized the catalytic hydrogenation of carbon dioxide. Considering the great progress achieved in this area, we feel it is necessary to contribute a new review paper, focusing on the recent advancements of methanation catalysts research and development. Also, the reaction thermodynamics, mechanism and kinetics, and the effects of catalyst active components, supports, promoters, and preparation methods will be reviewed and discussed. We hope this review will not only outline the achievements and technical problems, but also direct the future methanation catalysts design and development for SNG production.

2. Thermodynamics

During methanation, some side-reactions may occur which affects the purity of the SNG product. Table 1 lists the main possible reactions involved in the methanation process. Besides the normal methanation reactions (R1 and R2), carbon monoxide methanation reaction can also occur at lower H_2/CO ratio (R3).[21] The carbon monoxide disproportionation reaction (R4), also known as Boudouard reaction, is of great importance, since carbon on the catalyst surface is considered as a necessary intermediate during the methanation reaction.[22] In addition, water plays an important role through the water–gas shift reaction (R5), which would modify the surface and catalytic chemistry of methanation catalysts.[23] Among these reactions, it has to be noticed that R1, R2, and R4 can be regarded as three independent reactions. The other reactions can be described as a linear combination of these three reactions.

The equilibrium constants of the eight reactions involved in the methanation were calculated at different temperatures (Fig. 1).[24] It can be seen that all the reactions are favorable at low temperatures (<~400 °C) due to their exothermic characteristics. Obviously, low temperature and high pressure are preferred for carbon monoxide and carbon dioxide methanation. However, it is challenging to develop a catalyst that can achieve equilibration at low temperature for carbon monoxide and carbon dioxide methanation.[17,18]

Recently, we conducted a systematic thermodynamic analysis for methanation reactions of carbon oxides to produce SNG.[24] The effects of temperature, pressure, ratios of H_2/CO and H_2/CO_2, and the addition of other compounds in the feed gas on the conversion of carbon monoxide and carbon dioxide, methane selectivity and yield, as well as carbon deposition, were carefully investigated. The product composition distributions from stoichiometric carbon monoxide and carbon dioxide methanation reaction at equilibrium under 0.1 MPa are shown in Fig. 2a and b, respectively. For carbon monoxide methanation (Fig. 2a), the products mainly contain methane, water and little carbon dioxide by-product at low temperatures (200–300 °C) without deposition of carbon. With an increase in reaction temperature, the mole fraction of CH_4 decreases, whereas the unreacted carbon monoxide, hydrogen, carbon dioxide, and deposited carbon increase simultaneously.

Methane and water are the main products of carbon dioxide methanation (Fig. 2b) at low temperatures (200–250 °C). Noteworthily, the carbon dioxide methanation proceeds highly selectively as compared with the carbon monoxide methanation.[25] Raising the reaction temperature above 450 °C results in the increase of the carbon monoxide by-product, due to the reverse water–gas shift reaction, and meanwhile, unreacted carbon dioxide and hydrogen also increase, along with a decrease in the methane yield. The reduction of the fully oxidized carbon to methane is an eight-electron process with significant kinetic barriers, which thus requires a highly active catalyst to achieve acceptable rate and selectivity.[20] Through thermodynamic analysis, it is possible to obtain a useful guidance in the catalyst development and process control of methanation for the SNG production.

Table 1 Main possible reactions involved in methanation of carbon oxides, adapted from ref. 24 with permission of the Royal Society of Chemistry

Reaction no.	Reaction formula	$\Delta H_{298\ K}$ (kJ mol^{-1})	$\Delta G_{298\ K}$ (kJ mol^{-1})
R1	$CO + 3H_2 \leftrightarrow CH_4 + H_2O$	−206.1	−141.8
R2	$CO_2 + 4H_2 \leftrightarrow CH_4 + 2H_2O$	−165.0	−113.2
R3	$2CO + 2H_2 \leftrightarrow CH_4 + CO_2$	−247.3	−170.4
R4	$2CO \leftrightarrow C + CO_2$	−172.4	−119.7
R5	$CO + H_2O \leftrightarrow CO_2 + H_2$	−41.2	−28.6
R6	$2H_2 + C \leftrightarrow CH_4$	−74.8	−50.7
R7	$CO + H_2 \leftrightarrow C + H_2O$	−131.3	−91.1
R8	$CO_2 + 2H_2 \leftrightarrow C + 2H_2O$	−90.1	−62.5

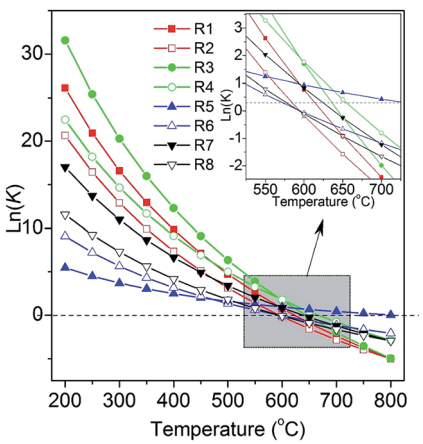

Fig. 1 The calculated equilibrium constants (K) of the eight reactions involved in methanation process. Adapted from ref. 24 with permission of the Royal Society of Chemistry.

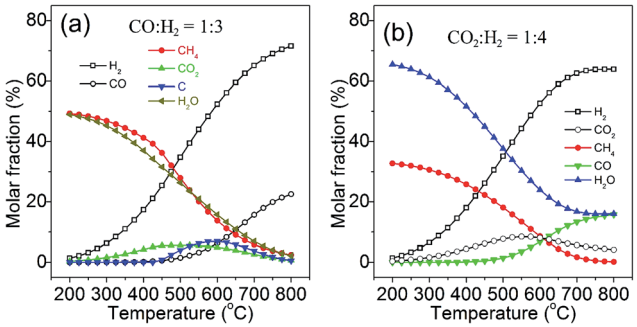

Fig. 2 Product compositions for CO (a) and CO_2 (b) methanation at equilibrium (0.1 MPa). Adapted from ref. 24 with permission of the Royal Society of Chemistry.

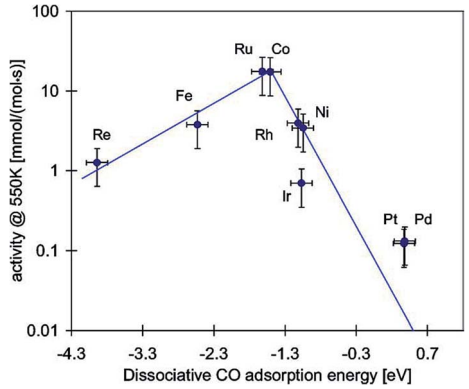

Fig. 3 Activities of different supported transition metal catalysts as a function of the reaction energy for dissociative carbon monoxide chemisorption. Reprinted from ref. 26, Copyright (2004), with permission from Elsevier.

3. Methanation catalysts

Methanation catalysts are typically composed of active metal particles dispersed on metal oxide supports. Up to now, a number of active metals including Ni, Fe, Co, Ru, Rh, Pt, Pd, W, Mo and various oxide supports (Al_2O_3, SiO_2, TiO_2, SiC, ZrO_2, CeO_2, $Ce_xZr_{1-x}O_2$) have been carefully investigated in both carbon monoxide and carbon dioxide methanation reactions for SNG production.

3.1 Active components

In 1975, Vannice M. A.[11] firstly compared the specific activity and product distributions of group VIII metals dispersed on Al_2O_3 in the synthesis of hydrocarbons from H_2–CO mixtures, and found that carbon monoxide methanation reaction could occur readily over these metals. The specific activity follows the order of Ru ≫ Fe > Ni > Co > Rh > Pd > Pt > Ir. It is well known that methanation reactions involve hydrogen, carbon monoxide and/or carbon dioxide adsorption and dissociation. The reaction rate of carbon monoxide methanation is closely related to carbon monoxide dissociation. Bligaard *et al.*[26] calculated the reaction energy for dissociative carbon monoxide adsorption at 550 K and compared it with the measured carbon monoxide methanation activities (Fig. 3). A clear volcano relationship was observed. The maximum of the volcano is approximately at a dissociative adsorption energy of −1.4 eV, which is in very good agreement with the prediction of Nørskov's results.[27] Although the sequence of activity in Fig. 3 is a little different from that of Vannice's results, noble metal Ru is undoubtedly the most active one for the methanation reaction. However, Ni catalysts draw more attention for methanation due to their relatively high activity and low price.

Table 2 and 3 list some carbon monoxide and carbon dioxide methanation catalysts studied in recent years. It should be noted that it is difficult to directly compare the performance of these catalysts because different reaction conditions were used. However, some general results can be summarized. Ni with loading amounts of 10–40 wt% is the main active metal for carbon monoxide methanation. Nearly 100% conversion of carbon monoxide and about 90–100% selectivity of methane could be obtained over optimized Ni catalysts at 3.0 MPa with H_2 : CO feed ratio of 3. Some Ni catalysts could maintain good activity over 100 h.[28–30] Even at 0.1 MPa, carbon dioxide methanation (Table 3) could still remain a high methane selectivity of nearly 100%, which is in accordance with the thermodynamic results.[24] However, high carbon dioxide conversion is difficult to reach at low temperatures because of the high kinetic barriers of the reaction processes. During catalyst activity testing, space velocity deeply affects the carbon monoxide and carbon dioxide conversion and methane selectivity. High space velocity is recommended to test the activity of methanation catalysts far from thermodynamic equilibrium.

3.1.1 Nickel. Nickel (Ni) has been applied as active component and promoter in catalysts for Fischer–Tropsch synthesis (FTS).[59] The main obstacle to its industrial application in FTS is the formation of volatile carbonyls, which cause deactivation of the catalyst and loss of active phase. In fact, Ni is better for methanation reaction to produce methane as compared with Co and Fe. Ni nanoparticles are usually dispersed on supports with high surface area as methanation catalysts, although unsupported Ni nanoparticles[60,61] or Raney® Ni[62] are also active for carbon monoxide and carbon dioxide methanation. The activity and selectivity of the supported Ni catalysts are strongly influenced by the amount of Ni metal loading,[31,63–65] the size of the dispersed Ni metal particles,[32,66–69] metal-support interactions,[70–72] and the composition of the support.[28,73,74] Ni supported on Al_2O_3 (Fig. 4) is one of the most widely studied catalysts in methanation reactions for the production of SNG due to its high performance-cost ratio.[29,75,76] Hu *et al.*[65] found that there existed three distinct active phases in Ni/Al_2O_3 when the nickel loading was less than 10 wt%, which originated from reduction of different nickel species at different reduction temperatures with each phase exhibiting different activity and mechanism for carbon monoxide and carbon dioxide methanation. Qin *et al.*[77] found that highly dispersed amorphous NiO after reduction was more active for methanation reaction because of its weaker interaction with the support and lower carbon monoxide dissociation energy. Carbon monoxide methanation reaction is highly structure sensitive.[78] The atomic step sites of Ni play important roles as

Table 2 Summary of the carbon monoxide methanation catalysts developed in recent years[a]

Catalysts	Preparation methods	Active metal content wt%	Catalytic performance					Stability test time/h	Ref.
			P/MPa	WHSV/(mL g^{-1} h^{-1})	*T*/°C	X_{CO}/%	S_{CH_4}/%		
Ni–Al_2O_3	CP	15	0.1	2500 h^{-1}	400	98.2	84.7	120*	1
Ni–Al_2O_3	Sol–gel	40	1.0	8160	230	96.5	76.8	—	31
Ni–Al_2O_3	I	10	0.1	240 000	450	61	68	50*	32
Ni–SiC	I	4.2	3.0	4006	500	96.7	100	120	28
Ni–Mg–Al_2O_3	I	20	0.1	30 000	400	100	80	196	29
Ni–Al_2O_3	I	10	3.0	30 000	400	97	90	10*	33
Ni–Mg–Al_2O_3	I	40	0.1	36 000	300	64	58	50	34
Ni–Mg–Al_2O_3	CP + HT	19	0.1	60 000	427	85	84	—	35
Ni–La_2O_3/Al_2O_3	I	15	1.5	10 000 h^{-1}	300	72	80	264	30
Ni–TiO_2	Sonication	23	0.1	38 800 h^{-1}	280	52	95	—	36
Si–Ni/SiO_2	Silicification	20	0.1	4800	350	50	28	42	37
Ni/MCM-41	HT	10	0.1	12 000	350	97.9	88.2	100	38
Ni/$CaTiO_3$	I	10	3.0	10 000	350	95	72	50	39
Ni/$BaO\cdot 6Al_2O_3$	I	40	3.0	30 000	350	81	92	50	40 and 41
Ni–Mo-MCM-41	I	10	0.1	12 000	280	100	80	100	42
Co_3O_4	CP	—	2.0	50 000 h^{-1}	300	99	—	—	43
Ni/$LaFeO_3$	I	30	1.0	3000 h^{-1}	340	90	48	55*	44

[a] I: impregnation; P: precipitation; CP: co-precipitation; SC: solution combustion method; HT: hydrothermal synthesis; * deactivation was observed.

the active sites for carbon monoxide methanation.[17] Ni with lower coordination numbers possesses more step sites and can be obtained in highly dispersed Ni/Al_2O_3.[79] He *et al.*[52] found that a surface defect-promoted Ni nanocatalyst with low coordination numbers (Fig. 5) exhibited simultaneously enhanced activity and stability for carbon dioxide methanation.

Although Ni catalysts are preferred in catalytic methanation reaction, there still exist some problems, such as carbon deposition, sintering, $Ni(CO)_4$ formation, and sulfur poisoning during SNG production.[80,81] Therefore, the stability of methanation catalyst is of great importance besides the activity and selectivity. It is well known that the deactivation of supported metal catalysts by carbon or coke formation is a serious problem in methanation process.[82] The typical causes are:[83] (1) polluting the active metal surface, (2) blocking the voids and pores of catalysts, (3) physical disintegration of the catalyst support. Till now, three types of carbon have been identified on Ni catalysts: pyrolytic, encapsulating and whisker carbon.[80] Thermodynamically, carbon formation in carbon monoxide methanation is more favorable as compared with carbon dioxide methanation under the same reaction conditions.[24] In addition, higher hydrocarbons in biomass-derived syngas could dramatically enhance the formation of the carbon whiskers at the Ni surface.[75] The nickel clusters were found to be associated with the formation of carbon whiskers, supporting a mechanism involving detachment of Ni from the catalyst support during whisker formation (Fig. 6).[84]

Table 3 Summary of the carbon dioxide methanation catalysts developed in recent years

Catalysts	Preparation methods[d]	Active metal content wt%	Catalytic performance					Stability test time/h	Ref.
			P/MPa	WHSV/(mL g^{-1} h^{-1})	*T*/°C	X_{CO_2}/%	S_{CH_4}/%		
Ni–$Ce_{0.5}Zr_{0.5}O_2$	I	10	3.0	30 000 h^{-1}	300	70	—	—	45
Ni–TiO_2	DP	15	0.1	2400 h^{-1}	218	50	99	—	46
Co/KIT-6	I	20	0.1	22 000	260	45	99	—	47
Ru–TiO_2	Barrel-sputtering	0.8	0.1	864	180	100	100	170	48
Ni–CeO_2	I	10	0.1	10 000 h^{-1}	300	~90	100	—	49
$Ni_{0.8}Mg_{0.2}O$@SiO_2	CP	—	0.1	60 000	250	78	99	100	50
Ni/MSN[a]	I	5	0.1	50 000	300	64.1	99.9	200	51
Ni/H–Al_2O_3[b]	HT	20	0.1	2400	234	50	—	252	52
Ni–Ru/γ-Al_2O_3	CP	Ni: 10; Ru: 1.0	0.1	9000 h^{-1}	350	70	—	100	53
Ru–CeO_2/Al_2O_3	I	2	0.1	10 000 h^{-1}	300	60	99	—	54
$Ce_{0.95}Ru_{0.05}O_2$	Combustion	—	0.1	45 000	450	55	99	—	55
Ni/MCM-41	HT	3	0.1	5760	400	56	96.1	—	56
Ni/MC γ-Al_2O_3[c]	I	20	0.1	9000	300	74	100	10	57
Co0.4Ni/SiO_2	I	10	0.1	13 200	300	58	—	—	58

[a] MSN = mesostructured silica nanoparticles. [b] H-Al_2O_3 = hierarchical flowerlike Al_2O_3 matrix. [c] MC = mesoporous nanocrystalline γ-Al_2O_3. [d] I: impregnation; CP: co-precipitation; HT: hydrothermal synthesis; DP: deposition–precipitation.

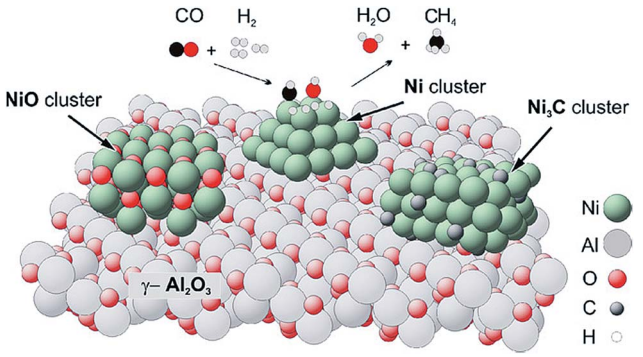

Fig. 4 Sketch of the catalyst structure and selective reactions occurring during the synthesis of methane. Reprinted from ref. 75, Copyright (2007), with permission from Elsevier.

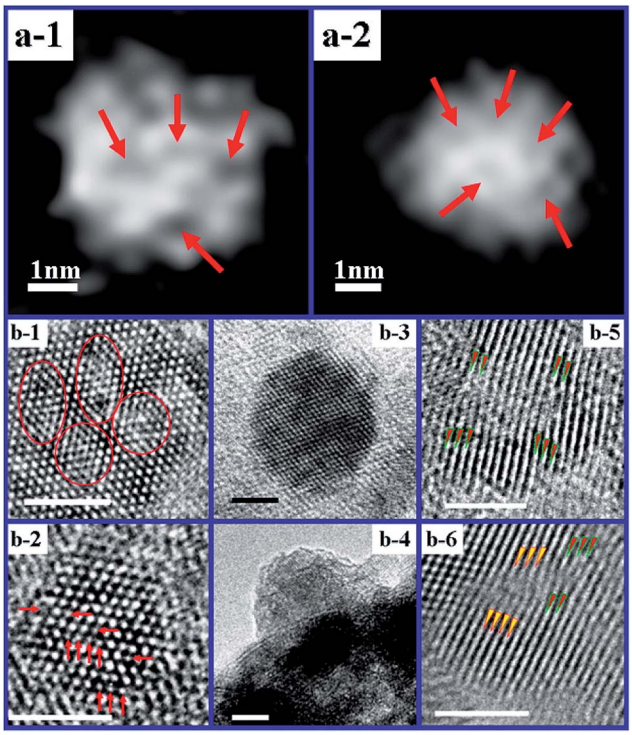

Fig. 5 (a-1 and a-2) High-angle annular dark field (HAADF) STEM images of Ni nanoparticles in Ni/H–Al_2O_3. (b-1–b-6) HRTEM images of Ni nanoparticles selected from the Ni/H–Al_2O_3 sample (the scale bar is 2 nm). Reprinted with permission from ref. 52 Copyright (2013) American Chemical Society.

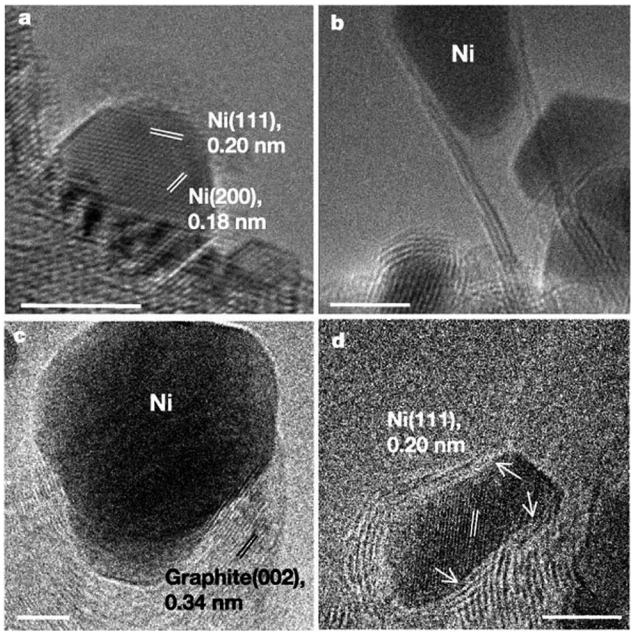

Fig. 6 Electron micrographs of the Ni catalyst and carbon nanofibres. (a) TEM image of a Ni nanocrystal supported on $MgAl_2O_4$. (b) TEM image showing a multi-walled tubular carbon nanofibre structure. (c) *In situ* TEM image showing a whisker-type carbon nanofibre. (d) *In situ* TEM image showing a Ni nanocrystal during carbon nanofibre growth. Scale bars, 5 nm. Reprinted by permission from Macmillan Publishers Ltd: [Nature] (ref. 84), Copyright (2004).

Prevention of catalyst deactivation caused by coke formation in the methanation of carbon oxides is critical. In summary, there are two ways to prevent the carbon formation: (1) optimization of operating conditions, such as adjusting reaction temperature or pressure, increasing the H_2/CO or H_2/CO_2 ratio, adding steam in the reactants.[85] (2) modification of catalysts by formation of an alloy,[86,87] and adding promoters like MgO,[29] CeO_2,[88] *etc.*

Ni nanoparticle sintering during the highly exothermic methanation process is another challenge for Ni catalysts. Jens Sehested from Haldor Topsøe conducted a lot of studies on this aspect.[89–92] Particle migration and coalescence, rather than Ostwald ripening was found to govern the sintering of Ni particles.[92] The proposed coalescence mechanism[89] explains the similar size of the sintered Ni particles independent of metal loading, and the rapid decrease in sintering rate with time. In addition, Sehested suggested a mathematical model that predicts well the experimental nickel surface area as a function of nickel loading, carrier surface area, temperature, and time.[90] This model not only enhances our fundamental understanding of the sintering phenomena, but also provides a tool for predicting metal surface areas of the used supported catalysts. What's more, the established formulas assuming that Ni_2–OH is dominating sintering[91] is a tool for predicting the sintering data and the performance of industrial catalysts.

In methanation process, water as a product could further accelerate the sintering process. In fact, even hot liquid water could lead to the structural changes of γ-Al_2O_3-supported catalysts.[93] Recently, Bai *et al.*[94] investigated the sintering of Ni/Al_2O_3 methanation catalyst in SNG production. Primary encapsulation of metallic nickel due to the collapse of the support structure and sporadic agglomeration of nickel crystallites led to the reduction of nickel surface area. The steam ambience induced formation of a Ni^{2+} doped alumina phase, further accelerated the loss of surface nickel atoms. More importantly, it has been found that the sintering could decrease the specific activity of nickel due to the surface structure change.[17]

Ni sintering can be slowed down by increasing the metal-support interaction,[38,56] adding promoters,[29,75,88,95] adopting improved preparation methods,[52,96] *etc.* recently, Lu *et al.* reported coking- and sintering-resistant palladium catalysts through atomic layer deposition of a thin Al_2O_3 protective layer,[87] which gave some inspirations in developing highly stable methanation catalysts.

When Ni methanation catalysts are operated at low temperatures (<250 °C) and high pressures, the formation of nickel tetracarbonyl ($Ni(CO)_4$) should be considered. Recently, Munnik *et al.*[66] investigated the stability of silica gel supported Ni catalysts during the carbon monoxide methanation reaction. The deactivation caused by Ostwald ripening was limited not by diffusion but due to the formation and decomposition of $Ni(CO)_4$ on metal surface, which were mainly determined by particle size. The supersaturation of $Ni(CO)_4$ was low in catalysts with medium sized nanoparticles (Fig. 7a and b), which limited the possible extent of their growth to the pore diameter (Fig. 8a and b). By contrast, in the case of small particles (Fig. 7c and d), the $Ni(CO)_4$ supersaturation was sufficiently high for the particles to break the pore walls, resulting in growth of very large nanoparticles (Fig. 8c and d).[66] Therefore, it seems that larger Ni nanoparticles (~10 nm) are more stable during low temperature carbon monoxide methanation process. Although the formation and decomposition of $Ni(CO)_4$ is not favorable in methanation reaction and should be avoided, this process can be used to modify the size of nickel particles and increase the dispersion of the metallic nickel phase in the Ni/ZrO_2 catalyst.[97]

Sulfur compounds (H_2S or thiophene (C_4H_4S)) are one of the major impurities in syngas which severely poison supported Ni catalysts.[98–100] Trace ammonia was also found to decrease the methanation catalyst activity *via* ammonia adsorption on the active catalyst sites in dynamic biogas upgrading process.[101] Even at ppm concentrations, sulfur compounds could still irreversibly affect the catalytic activity.[102] The adsorption of S blocks the active sites as well as accelerates the sintering and the oxidation of Ni^0 particles.[103] Legras and co-workers[99] studied the impact and detailed action of sulfur in syngas methanation on $Ni/\gamma\text{-}Al_2O_3$ catalyst. It was found that sulfur atoms preferentially adsorbed on the sites for reversible adsorption of molecular CO under the methanation conditions. The sites responsible for CO dissociation, which leads to CH_4 production, are affected to a lesser extent by sulfur poisoning (Fig. 9).

Several strategies have been adopted to improve the sulfur resistance of Ni catalysts. For example, the application of plasma decomposition, which led to the obtained catalyst with less defect sites on Ni particles, could enhance H_2S resistance for methanation of syngas.[104] In addition, the S adsorption could be weakened when S bound to both Ni and Ru atoms simultaneously. Therefore, $Ni\text{–}Ru/SiO_2$ catalyst with small bimetallic Ni–Ru particles showed enhanced sulfur tolerance.[103] However, the applications of these methods are still limited. How to increase the sulfur resistance of Ni methanation catalysts still requires further investigation.

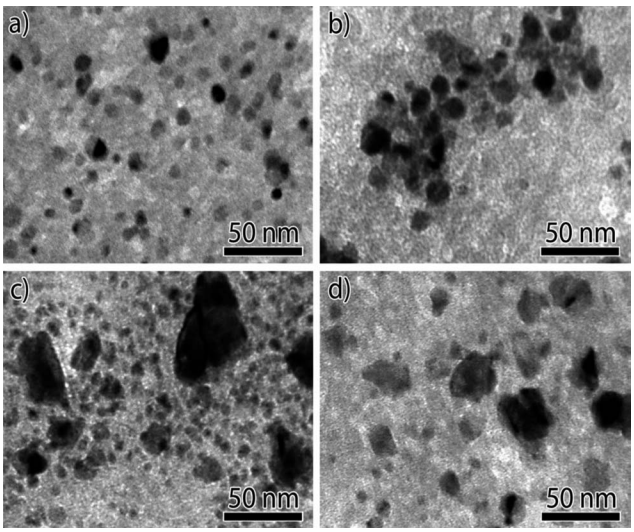

Fig. 8 TEM images of Ni/SiO_2 catalysts with different Ni particle sizes after 150 h on-stream (230 °C, H_2 : CO = 2 : 1, 0.1 MPa). (a) ~8 nm, (b) ~9 nm, (c) ~4 nm, and (d) ~3 nm. Reproduced with permission from ref. 66 Copyright (c) [2014 WILEY-VCH Verlag GmbH & Co. KGaA, Weinheim].

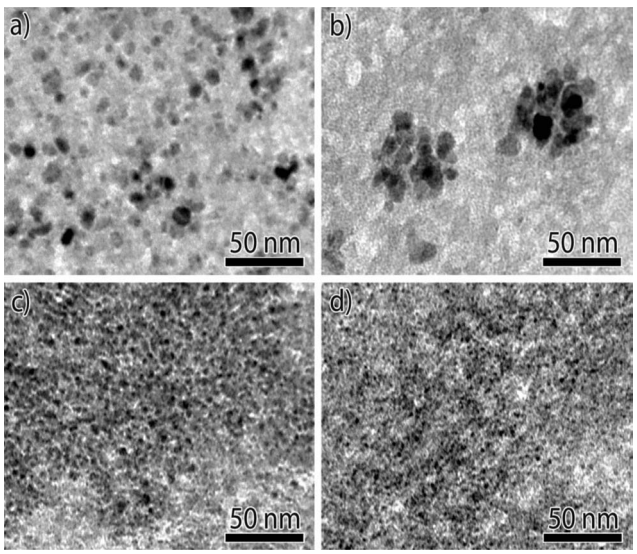

Fig. 7 Bright-field TEM images of Ni/SiO_2 catalysts with different Ni particle sizes after reduction: (a) ~8 nm, (b) ~9 nm, (c) ~4 nm, and (d) ~3 nm. Reproduced with permission from ref. 66 Copyright (c) [2014 WILEY-VCH Verlag GmbH & Co. KGaA, Weinheim].

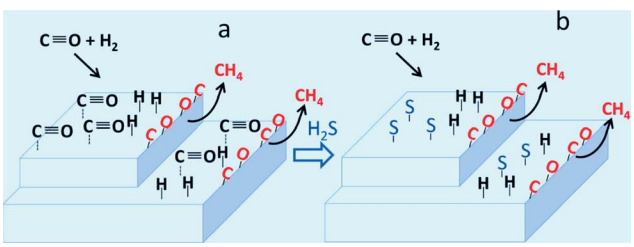

Fig. 9 Carbon monoxide hydrogenation with sulfur-free syngas (a) and with syngas containing small amounts of sulfur (b). Reproduced with permission from ref. 99 Copyright (2014) American Chemical Society.

3.1.2 Cobalt and iron. Co and Fe are also active for methanation reaction. Some studies[105–107] showed that higher methane selectivity could be observed in FTS when Co catalysts were not completely reduced or contained small Co_3O_4 particles. Zhu *et al.*[43] synthesized nanosized Co_3O_4 catalysts for low-temperature methanation of carbon monoxide in COG. The smaller nanosized (20 nm) Co_3O_4 catalysts showed higher carbon monoxide adsorption capacity. 100% CO conversion at temperatures as low as 180 °C and space velocity of 5000 h^{-1} could be achieved. When Co is dispersed on support, the structure of the support also affects the dispersion of Co species and thus the performance of Co-based catalysts.[47] Mesoporous Co/KIT-6 showed better carbon dioxide methanation catalytic performance compared with Co/meso-SiO_2 catalysts due to the highly ordered, bicontinuous, mesoporous structure of KIT-6. Co can also be used as promoters in methanation catalysts. The addition of cobalt species could improve the catalytic activity of MoO_3/Al_2O_3 catalyst toward sulfur-resistant methanation.[108] In addition, Co can further be combined with Ni[58,109–112] or Pt[113] to form bimetallic methanation catalysts, which showed higher methane yield as compared with single metal counterparts. The Co : Ni ratio has significant effects on activities of bimetallic catalysts over different supports, such as Al_2O_3 and $CeZrO_x$.[58,109,111,112] Alayoglu *et al.*[113] studied the Co–Pt bimetallic nanoparticles supported on MCF-17 and found that Pt could promote the reduction of Co to its metallic state, resulting in different catalytic performance as compared with pure Co nanoparticles. Tuxen *et al.*[114] demonstrated that the dissociation of carbon monoxide on Co nanoparticles could be facilitated by hydrogen, which was also size-dependent. It was suggested that the dissociation occurred through a –COH or $–CH_xO$ intermediate, however, such intermediates were not directly identified. A clear size-dependent dissociation of carbon monoxide on Co nanoparticles was also observed, with smaller nanoparticles favoring molecular adsorption of carbon monoxide and larger nanoparticles favoring carbon monoxide dissociation (Fig. 10). Importantly, the ability of the nanoparticles to dissociate hydrogen determines their ability to dissociate carbon monoxide *via* the hydrogen-assisted mechanism, which was also supported by the density functional theory (DFT) calculations.[115]

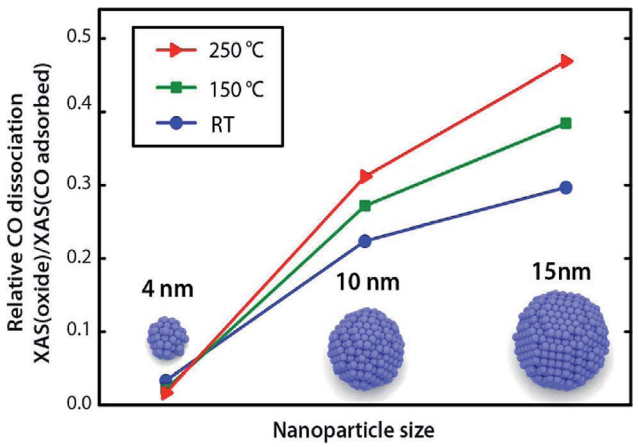

Fig. 10 Relative concentrations of dissociated CO species on 4, 10, and 15 nm nanoparticles after exposure to CO/He at different temperatures. Reproduced with permission from ref. 114 Copyright (2013) American Chemical Society.

In general, pure Fe has low methanation activity and selectivity to methane. However, when combined with Ni, in the form of Ni–Fe bimetal or alloy, it showed high activity for methanation[44,63,116–118] and even surpassed monometallic Ni catalysts. Hwang and co-workers compared different second metal addition on the activity of nickel–M–Al_2O_3 (M = Fe, Co, Ce, La, Zr, Y, Mg) catalysts for carbon monoxide or carbon dioxide methanation. Among which, Fe exhibited the best promotional effect.[110,119] Co and/or Fe can be combined with Ni to form enhanced methanation catalysts, however, their synergistic effect needs further study to understand the reaction mechanism.

3.1.3 Ruthenium. Ru catalysts are very active for methanation and can have high activities even at low temperatures.[55,68,120,121] Abe *et al.* reported 100% yield of CH_4 at 160 °C on a 0.8 wt% Ru/TiO_2 catalyst with Ru diameter of 2.5 nm.[48] This catalyst showed no deactivation over at least 170 h test. It was concluded that the size of Ru nanoparticles determined the hydrogenation activity. However, no smaller Ru nanoparticles were investigated to figure out if the methanation activity could be further enhanced. Masini *et al.*[122] found that the turnover frequency of carbon monoxide methanation increased with mass-selected Ru nanoparticles with diameters of 4–10 nm on a planar SiO_2 model support. Lowly coordinated sites of Ru are important for the high activity. Carbon deposition and possible surface restructuring are the causes for activity loss over repeated reactions. However, DFT simulations suggest that carbon monoxide is activated predominantly *via* H-assisted paths on high-coordination Ru atoms in (111) terrace environments on carbon monoxide chemisorption and dissociation during carbon monoxide hydrogenation on Ru catalysts.[123] Ru cluster size also affects the product selectivity during carbon dioxide reduction with H_2.[124] When Ru is mostly atomically dispersed on the Al_2O_3 support, carbon monoxide is formed with high selectivity. With increasing Ru particle size, the selectivity toward methane formation is increased, while that toward carbon monoxide production is decreased.

Ru can also be combined with Ni to form a bimetallic methanation catalyst, which showed much enhanced performances.[53,103] Zhen *et al.*[53] found that the segregation of Ru on the Ni–Ru/γ-Al_2O_3 catalyst surface could provide more active Ru species and possess better sulfur-tolerance. Therefore, adding small amount of Ru in Ni catalyst is a promising way to promote methanation reaction.[125] Long time stability, high activity, and low loading account for the crucial factors which lead to the use of the precious metal Ru in SNG production.

3.1.4 Rhodium, palladium, platinum, molybdenum. Other noble metals like Rh, Pd, Pt have also been studied for carbon oxides methanation. The nature of supports influences the activity and selectivity of Pd catalysts in carbon monoxide hydrogenation. For example, Pd/TiO_2 mainly produces methane.[126] Higher carbon monoxide conversions over Pd/ZrO_2

and Pd/TiO_2 were ascribed to the presence of cationic Pd species formed through the metal-support interaction.[71,127] Shape-controlled Pd nanoparticles embedded in mesoporous silica (Fig. 11) were also tested in carbon dioxide hydrogenation.[128] It was found that Pd crystallographic surface orientation and the corresponding mean coordination number of surface atoms played an important role in the adsorption strength of reactants and intermediate species, thus influencing their surface coverage, and finally the activity and selectivity.

Pt dispersed on mesoporous silica showed poor activity towards carbon monoxide methanation.[113,129] However, the catalytic activity of Pt could be significantly improved by depositing Pt on metal oxide supports through the well-known strong-metal-support-interaction effects,[130] and TiO_2 nanotube supported Pt shows high activity for carbon dioxide methanation.[131] Similarly, CeO_2 supported or promoted Rh catalysts[132,133] also showed high activity for carbon dioxide methanation.[134]

Mo has relatively low activity for methanation and produces primarily non-methane hydrocarbons. Consequently, most studies of Mo catalysts have focused on MoO_x and MoS_x in sulfur-resistant methanation.[135,136] The structure and resistance to carbon monoxide of Mo and MoO_3 have been well reviewed.[137] Unsupported MoS_2 were used as sulfur-resistant carbon monoxide methanation catalyst and showed high activity.[138] MoO_x could promote Ni catalysts for carbon monoxide or carbon dioxide methanation both physically and electronically.[42,139] In particular, the effects of CeO_2–Al_2O_3 composite support[73,140,141] and sulfidation process[142–144] on MoO_3/Al_2O_3 catalysts for sulfur-resistant methanation were intensively investigated. The main factors controlling SNG production by methanation of syngas in the presence of sulfur-resistant Mo-based catalysts were also determined.[145] Mo based catalysts show high potential for sulfur-resistant methanation and more attention should be paid to further increase their activities.

3.2 Supports

Support plays an important role in the performance of a heterogeneous catalyst, which usually affects the metal-support interaction and metal dispersion, hence further influences the activity, selectivity, and stability of a catalyst.[126] Till now, various metal oxides (Al_2O_3, SiO_2, ZrO_2, TiO_2, CeO_2 *etc.*), composite oxides (hexaaluminate, solid solution, perovskite) and SiC have been used as methanation catalyst supports. Of all these materials, Al_2O_3 is the most typical one for methanation reaction.

3.2.1 Al_2O_3. Active Al_2O_3 serves as an excellent support material and/or catalyst for many industrial processes. The chemistry of Al_2O_3 is more complicated than that of other metal oxides such as SiO_2, TiO_2, due to various crystallographic modifications (like γ, κ, δ, θ, α phase).[146] γ phase Al_2O_3 has been widely investigated due to its high surface area, developed pore structure and well-characterized surface acid–base properties.[147] Recently, we compared the performance of supported Ni catalysts on commercial γ-Al_2O_3 with different properties for carbon monoxide methanation.[29] The results showed that the properties of γ-Al_2O_3 strongly affected the catalytic performance. Ni supported on mesoporous nanocrystalline γ-Al_2O_3 with ordered structure showed increased activity and stability for carbon dioxide methanation.[57] The effects of the structures and surface properties of Al_2O_3 supports calcined at different temperatures on the catalytic performances of Ni/Al_2O_3 catalysts were also investigated.[33] Calcination above 1000 °C yields crystalline, non-porous, stable α-Al_2O_3 support, which can be used as a low-surface-area support material.[32,33] However, α-Al_2O_3 is not a good support to stabilize nickel nanoparticles.[148] The main problem of Al_2O_3 support during methanation reaction is the sintering in the presence of water (a product of methanation reaction) at high temperature. To increase the stability of Al_2O_3 support, a series of promoters

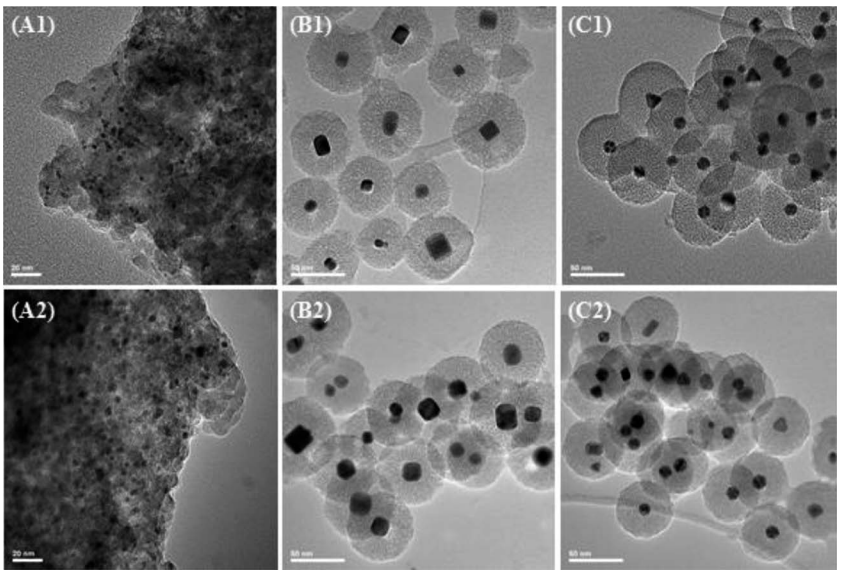

Fig. 11 TEM images of Pd_{imp}/SiO_2 (A), $Pd_{cub}@SiO_2$ (B) and $Pd_{pol}@SiO_2$ (C) catalysts before (1) and after (2) catalytic test. Reproduced from ref. 128 Copyright (2015), with permission from Elsevier.

such as MgO, La_2O_3, CeO_2 have been added in methanation catalysts, which will be discussed later in Section 3.3.

3.2.2 SiO_2, TiO_2, ZrO_2, CeO_2. SiO_2 as a catalyst support is usually in amorphous form. One major advantage of SiO_2 over other support materials is the ease of adjustment and control of the mean pore diameter, the specific surface area and pore volume. SiO_2 supported catalysts have been widely studied in methanation reactions.[51,74,149–151] Catalyst preparation methodologies have a significant effect on the activity and stability of Ni/SiO_2 catalyst for syngas methanation. For example, catalyst prepared by plasma decomposition resulted in high dispersion of Ni, enhanced interaction between Ni and the SiO_2 support, as well as less defect sites on Ni particles[149,150] which showed high activity and enhanced sulfur-resistance.[104] Si–Ni intermetallic compounds supported on SiO_2 exhibited high activity for carbon monoxide methanation.[37] Similar to Al_2O_3, how to increase the hydrothermal stability of SiO_2 under methanation process still requires further investigation.

TiO_2 as a useful semiconductor material has been widely studied in photocatalysis.[152] As the methanation catalyst support, TiO_2 supported Ni catalysts have shown high activity for methanation reactions. Partial substitution of Ni in TiO_2 lattice could be achieved through sonication, which creates oxide vacancies and facilitates hydrogen adsorption and spillover from nickel to support, further increases catalytic performance.[36] In addition, different from Al_2O_3 support, electron transfer from TiO_x could increase the electron cloud density of Ni atoms, which in turn could promote carbon monoxide dissociation on the catalyst surfaces, leading to a relatively high catalytic performance.[153,154]

ZrO_2 support is similar to TiO_2 which could improve the dispersion of Ni as well the hydrogen-promoted dissociation of carbon monoxide.[155] High carbon monoxide or carbon dioxide methanation activities were obtained on MoS_2/ZrO_2,[156] Yb_2O_3 doped Ni–ZrO_2 catalysts[157] and mesoporous ZrO_2 supported Ni catalysts.[158,159]

CeO_2 is a special catalyst support because of its partially reducing properties.[160–163] Ni/CeO_2 showed high carbon dioxide conversion and CH_4 selectivity as compared with Ni/α-Al_2O_3, Ni/TiO_2, and Ni/MgO in CO_2 methanation reaction.[49] It is well established that Ce has the ability to undergo rapid transformations between Ce^{4+} and Ce^{3+} states under oxidizing and reducing environments.[161,164] The bulk vacancies created in CeO_2 after reduction at high temperature could enhance the carbon dioxide methanation activity.[134] Ni coverage on CeO_2(111) surfaces also affects the carbon monoxide methanation activity.[88,165] In addition, combining CeO_2 with ZeO_2 to form $Ce_xZr_{1-x}O_2$ solid solution could lead to improved support properties such as high redox property, excellent thermal stability, resistance to sintering and suppressing coke formation.[45,109,112,166,167]

3.2.3 SiC, hexaaluminate, perovskite. SiC as a potential catalyst support has received increasing attention in recent years due to its excellent thermal conductivity, good chemical inertness, and high mechanical strength.[168,169] SiC supported Ni catalysts showed good activity and selectivity in syngas methanation.[28,170–174] Additionally, Ni/SiC exhibited higher resistance to sintering and carbon deposition and is easier for regeneration than Ni/Al_2O_3 (ref. 28) and Ni/TiO_2 (ref. 171) due to the high thermal conductivity of SiC. Further investigation[170] showed that proper oxidation of the SiC support could obtain active silicon oxides which could disperse and strongly anchor Ni particles to enhance both the low-temperature activity and the high-temperature stability of the catalysts.

Hexaaluminate type materials possess a unique layered structure with alternative stacked spinel blocks separated by mirror planes. We investigated Ni catalysts supported on barium hexaaluminate (Ni/BHA) for carbon monoxide methanation.[40,41] Compared with Ni catalysts supported on commercial Al_2O_3, the Ni/BHA catalysts exhibited much higher catalytic activity and thermal stability, as well as stronger resistance to carbon deposition.

Perovskite oxides have been widely used in high temperature reactions[175] due to their high thermal stability, good reactivity of lattice oxygen, and low cost.[176] $CaTiO_3$ supported Ni catalyst and $LaFeO_3$ supported Ni–Fe catalyst showed better catalytic performances than Ni/Al_2O_3 in carbon monoxide methanation.[39,44]

Other supports such as rice husk ash,[177–179] mesoporous zirconia-modified clays,[180] and carbon[181] have also been used in methanation catalysts and showed high activity. Generally speaking, the ideal methanation catalyst support needs to be stable at high temperature under steam ambience, with high surface area to disperse active metal, and with appropriate surface properties to effectively anchor active metal nanoparticles.

3.3 Promoters

Promoters can be mainly classified as two types: (1) electron promoter to change the electron mobility of catalyst. (2) Structure promoter to improve the dispersion and thermal stability of catalyst by changing the chemical component, crystal texture, pore structure, dispersion state, and mechanical strength of catalyst. Some oxide promoters can serve with both functions.

MgO is an effective promoter to improve resistance to carbon deposition and to minimize Ni particles sintering.[29,182–185] MgO promoted Al_2O_3 ($Mg_2Al(O)$) supported with Ni[184] and Ni/Mg/Al hydrotalcite-like compounds[186] showed excellent catalytic activity and thermal stability in methanation reaction, which demonstrates the effectiveness of adding promoters to tailor the properties of composite oxide catalyst support to improve the catalyst thermal stability for efficient SNG production.

La_2O_3 addition can restrain the growth of NiO particles, increase the H_2 uptake and Ni dispersion, and therefore enhance the activity of catalysts.[30,187,188] Tada *et al.*[189] found La-electron-promoter could increase the electron density in Ru species, which enhanced the dissociation of the C–O bond on Ru due to back donation of electrons from Ru to carbon monoxide, hence led to high carbon monoxide methanation activity over Ru–La/TiO_2. The addition of CeO_2 can improve the reducibility of the methanation catalyst by altering the interaction between Ni and Al_2O_3.[54,88,190,191] The Pt doping also can facilitate the reduction of Ni species.[129] TiO_x species[153,192] and ZrO_2 (ref. 155 and 193) were found to effectively restrict the formation of $NiAl_2O_4$ spinel phase and weaken the Ni–Al_2O_3

interaction, leading to a higher exposure of Ni species and thus enhancing the carbon monoxide adsorption capacity. In addition, electron transfer from TiO_x could increase the electron cloud density of Ni, which facilitates the dissociation of CO.[153] The same phenomenon was also found in MoO_3 promoted Ni methanation catalysts.[42] Zr doping improved the dispersion of Ni as well as hydrogen-promoted dissociation of carbon monoxide. Most recently, addition of V_2O_3 was found to enhance the activity and coking resistant of Ni–Al_2O_3 for carbon monoxide and carbon dioxide methanation due to the formation of $Ni_3V_2O_8$.[194] Na could also promote Ni/γ-Al_2O_3 catalysts for syngas methanation.[195] Till today, a lot of research efforts have been made towards searching for new promoters to improve the performance of the methanation catalysts. However, a magic promoter seems not to be in sight yet.

3.4 Preparation methods

Various methods have been investigated for preparing methanation catalysts. Preparation methods affect the dispersion of active metal[68] and metal-support interactions,[196] which in turn further influences the catalytic performance.[197] Traditional methods including impregnation,[28,30,40,41,45,170,171,193,198,199] precipitation,[43,95,109,157,200] and sol–gel methods[31,63,110,201] have been widely applied in methanation catalysts synthesis. Some other methods such as deposition–precipitation,[46,142] hydrothermal synthesis,[38,202] ion exchange method,[203] mechanical mixing,[204] solution combustion method,[96] and microwave heating[77] were also used in preparing methanation catalysts.

Previous studies[205,206] showed that co-precipitated Ni–Al_2O_3 catalysts could obtain a high dispersion of active metal and strong metal-support interaction, which exhibited higher stability for methanation at high temperatures as compared with those obtained through the impregnation method. The precipitants (such as NH_4OH, NaOH, $(NH_4)_2CO_3$, and Na_2CO_3) used in co-precipitation strongly influenced the activity of Ni–Mg/Al_2O_3 catalysts in syngas methanation[182] and NiFeAl catalysts in carbon dioxide methanation.[117] In addition, the activities of Ni–Ru bimetallic catalysts for carbon dioxide methanation are highly dependent on the precipitation sequence during co-precipitation.[53] Similarly, the Mg-modified Ni/SiO_2 catalysts prepared by co-impregnation method showed better activity and stability than those prepared by sequential impregnation method.[183] O'Brien and co-workers[207] studied the active phase evolution in single Ni/Al_2O_3 methanation catalyst prepared by impregnation in real time using combined μ-XRD-CT and μ-absorption-CT. Both the oxidation procedure and the spatial distribution/concentration of the Ni just prior to oxidation affected the distribution of active Ni metal. Some new methods were also applied in methanation catalysts preparation to enhance the catalytic performance. For example, plasma treatment remarkably improved the dispersion of active components and enhanced the reactivity of Ni/SiO_2 catalyst.[149] The dielectric-barrier discharge plasma decomposition resulted in a higher dispersion of Ni, an enhanced interaction between Ni and the SiO_2 support, as well as fewer defect sites on Ni particles that could enhance resistance to sintering and sulfur poisoning.[104,150] It should be noted that the pretreatment/activation process can also affect the final performance of the methanation catalysts.[159,166,208]

4. Reaction mechanisms and kinetics

4.1 CO methanation

The mechanism of carbon monoxide hydrogenation has been examined under conditions of the FTS.[209] Molecular level studies have revealed how the activated dissociation of hydrogen and carbon monoxide occurs.[23] Generally, the dissociation of hydrogen on transition metal surfaces is facile. Carbon monoxide methanation process is initiated through carbon monoxide dissociation, and hence, a fundamental understanding of carbon monoxide activation is of utmost importance. Extensive experimental and theoretical studies[78,210–212] have been carried out to investigate the reaction pathways of carbon monoxide dissociation and to identify the active sites responsible for the low carbon monoxide dissociation barrier. These studies have confirmed that the active sites present along stepped and corrugated metal surfaces could reduce the carbon monoxide dissociation barrier. In principle carbon monoxide dissociation may occur through one of three pathways:[211,212]

$$CO_{ads} + * \rightarrow C_{ads} + O_{ads} \quad (1)$$

$$CO_{ads} + H_{ads} \leftrightarrow HCO_{ads} + * \rightarrow HC_{ads} + O_{ads} \quad (2)$$

$$CO_{ads} + H_{ads} \leftrightarrow COH_{ads} + * \rightarrow C_{ads} + OH_{ads} \quad (3)$$

Two mechanisms for carbon monoxide activation have been hypothesized. One suggests that the carbon monoxide dissociation directly (path a) follows hydrogenation to produce CH_x species. The other proposed mechanism is that the carbon monoxide dissociation proceeds through hydrogen-assisted intermediates (path b and c). Shetty's results[212] demonstrate that the direct carbon monoxide dissociation on corrugated Ru(1121) surface has a lower overall barrier than the hydrogen-assisted carbon monoxide pathways, which is due to the highly endothermic steps to form the intermediates during the hydrogenation paths. However, Ojeda *et al.*[213] found that, by using theoretical analysis, the unassisted CO* activation was not competitive with the H-assisted route in Co catalysts, leading to oxygen rejection pathways exclusively. This study provided both experimental and theoretical evidences for hydrogen-assisted carbon monoxide activation as the predominant kinetically relevant step on Fe and Co catalysts. HCO_{ad} was also identified as reaction intermediate species in the dominant reaction pathway for carbon monoxide methanation on Ru/Al_2O_3 catalyst,[214] but no such species was detected on Ru/zeolite. Panagiotopoulou *et al.*[215] provided evidences that methanation of carbon monoxide on Ru/TiO_2 occurs *via* two distinct reaction pathways: the first one involves hydrogenation of surface carbon produced by dissociative adsorption of carbon monoxide at low reaction temperatures, whereas the second one involves hydrogenation of Ru_x–CO species. Although

Table 4 Mechanisms proposed for carbon dioxide hydrogenation to methane. (a) H-assisted carbon monoxide dissociation. (b) Un-assisted carbon monoxide dissociation. Reproduced with permission from ref. 223 Copyright (2013), with permission from Elsevier

(a) H-assisted carbon monoxide dissociation	(b) Unassisted carbon monoxide dissociation
1. $CO_2 + 2^* \leftrightarrow CO^* + O^*$	1. $CO_2 + 2^* \leftrightarrow CO^* + O^*$
2. $H_2 + 2^* \leftrightarrow 2H^*$	2. $H_2 + 2^* \leftrightarrow 2H^*$
3. $CO^* + 2H^* \leftrightarrow H_2CO^* + 2^*$	3. $CO^* + ^* \rightarrow C^* + O^*$ (RDS)
4. $H_2CO^* + ^* \rightarrow CH^* + OH^*$ (RDS)	4. $C^* + H^* \leftrightarrow CH^* + ^*$
5. $CH^* + 3H^* \leftrightarrow CH_4 + 4^*$	5. $CH^* + 3H^* \leftrightarrow CH_4 + 4^*$
6. $O^* + H^* \leftrightarrow OH^* + ^*$	6. $O^* + H^* \leftrightarrow OH^* + ^*$
7. $OH^* + H^* \rightarrow H_2O + 2^*$	7. $OH^* + H^* \rightarrow H_2O + 2^*$

debates about the mechanism of carbon monoxide methanation (direct dissociative adsorption *vs.* H-assist CO dissociation) still exit, it seems that the reaction pathway differs with different active metal sites and reaction conditions.

The kinetics of carbon monoxide methanation reaction has been extensively studied under different conditions, and various reaction rate expressions have been proposed.[216–222] I. Alstrup[216] proposed a kinetic model based on carbon monoxide dissociation and stepwise hydrogenation of surface carbon. Hydrogenation of surface methylidyne was considered as the rate-controlling step, which is consistent with the results of Goodman *et al.*[217] and Polizzotti *et al.*[218] later, Sehested *et al.*[219] investigated the carbon monoxide methanation reaction over nickel, and the kinetics of this reaction could be well described by a first-order expression with carbon monoxide dissociation at the nickel surface. The first-order rate constant for CO* dissociation was 5×10^{-9} (s^{-1}) exp[−96.7 (kJ mol^{-1})/RT] assuming that 5% of the nickel surface atoms are active. Kopyscinski *et al.*[220] applied spatially resolved concentration and temperature measurements in a catalytic plate reactor for the kinetic study of carbon monoxide methanation. Three kinetics equations were obtained based on three different rate-determining steps (C* + H* → CH* + *, CH* + H* → CH_2* + *, COH* +

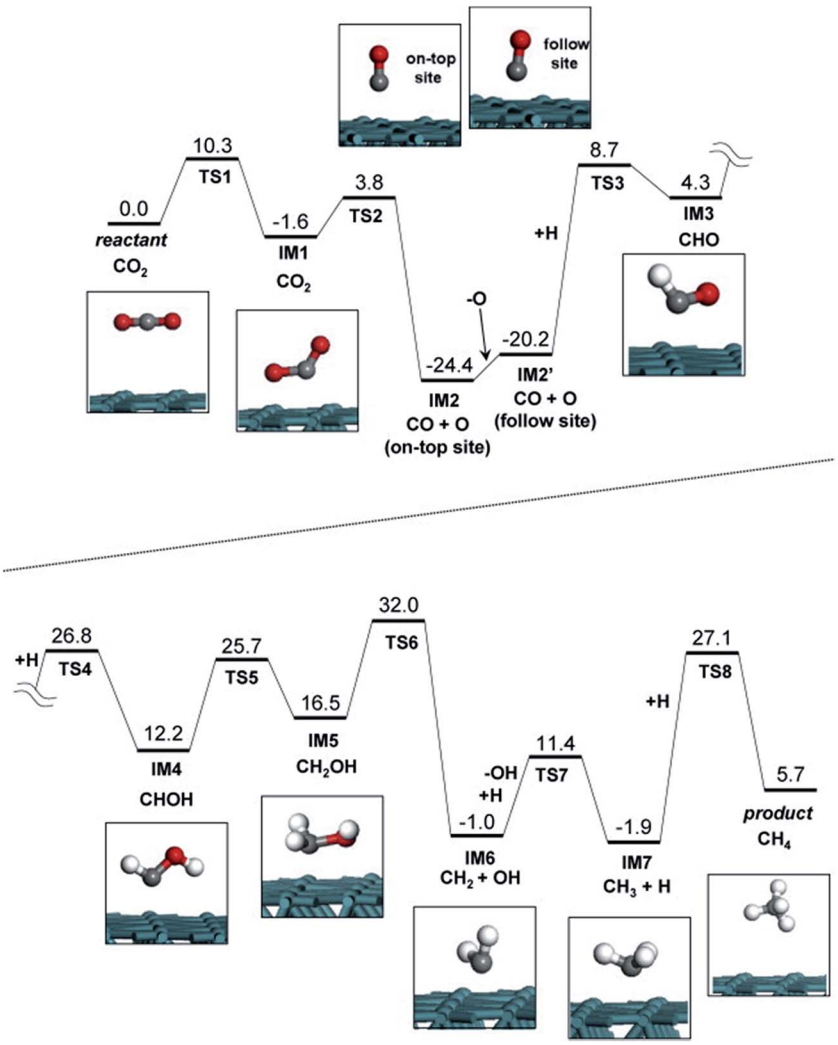

Fig. 12 Potential energy diagram for carbon dioxide methanation on the Ru surface slab structure. Each reactant, product and intermediate structures are also shown in the inset of the figure. Reproduced with permission from ref. 224 Copyright (2014), with permission from Elsevier.

H* → CH* + OH*, * empty active site). Interestingly, all three models reflected the measured data equally well and the activation energy of the methanation reaction was 74 kJ mol^{-1}. Transient experiments or spectroscopic methods are needed for further discrimination of the models. Zhang and co-workers investigated the kinetics of carbon monoxide hydrogenation under realistic conditions of methanation of biomass derived syngas.[221] The reaction rates were fitted by two kinetic models with hydrogenation of adsorbed carbon species as the rate limiting steps. The validated models could be used for modeling the realistic methanation process of biomass-derived syngas to predict the catalyst performance and to better determine the operation conditions.

4.2 CO_2 methanation

Even though the reaction mechanism of carbon dioxide methanation has been intensively investigated, there are still arguments on the nature of the intermediate compounds involved in the process and on the methane formation scheme.[214,223–227] The main discrepancy is whether the reaction goes through the formation of carbon monoxide intermediate.[214,223,225–227] Eckle and co-workers[214] studied the reaction intermediates and side products in the methanation of carbon monoxide and carbon dioxide over supported Ru catalysts. It was found that carbon dioxide methanation proceeded *via* dissociation to CO_{ad}, which was subsequently methanated. Formation and decomposition of surface formate only played a minor role in the carbon dioxide methanation reaction.

Recently, Karelovic *et al.* studied low temperature carbon dioxide methanation over Rh/TiO_2 catalysts.[223] Two reaction mechanisms (Table 4) were proposed based on carbon monoxide intermediate. On the basis of a kinetic comparison between two proposed reaction paths, it was concluded that the dissociation of $CO_{(ads)}$ could proceed *via* a H-assisted path, probably by the formation of Rh carbonyl hydride species. These results reveal the similarities of the reaction path and the metal particle size dependence between carbon dioxide and carbon monoxide hydrogenations.

Akamaru *et al.*[224] carried out a DFT analysis of methanation reaction of carbon dioxide on Ru nanoparticle supported on TiO_2 (101). The potential energy diagram is shown in Fig. 12. The adsorbed carbon dioxide on each site can transform into carbon monoxide through different reaction paths with nearly the same potential energy barriers.

Aldana *et al.*[225] investigated carbon dioxide methanation mechanism over Ni-based ceria–zirconia catalysts. Different from the above results, H_2 was found to dissociate on Ni^0 sites while carbon dioxide was activated on the ceria–zirconia support to form carbonates which could be hydrogenated into formate and further into methoxy species (Fig. 13). This mechanism involves weak basic sites of the support for the adsorption of carbon dioxide and implies a stable metal-support interface, which explains the much better activity of these catalysts as compared to Ni–silica on which both carbon dioxide and hydrogen are activated on Ni^0 particles. Pan *et al.*'s results also support this mechanism.[226,227]

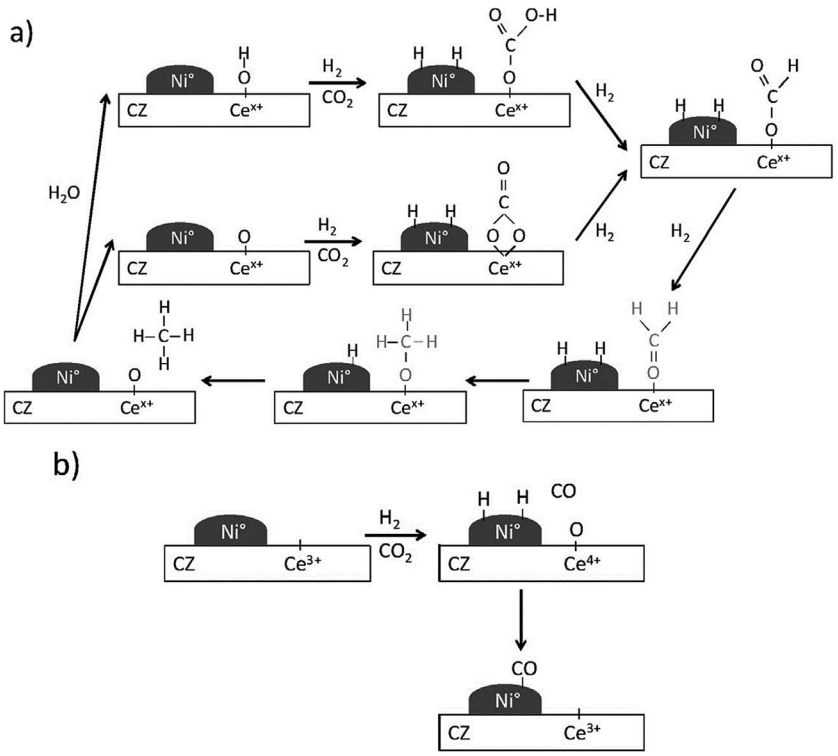

Fig. 13 Reaction mechanism proposed on Ni–CZ sol–gel sample for: (a) carbon dioxide methanation and (b) carbon monoxide formation. Reproduced with permission from ref. 225 Copyright (2013), with permission from Elsevier.

Park and co-workers proposed a bifunctional mechanism in Pd–Mg/SiO_2 catalysts for CO_2 methanation:[228] carbon dioxide is stabilized by the magnesium-containing oxide as a surface carbonate and sequentially hydrogenated to form methane.

The methanation kinetics of carbon dioxide was also investigated in recent years.[124,229,230] Lu and Kawamoto investigated CO_2 methanation kinetics over mesoporous silica incorporated with Ni catalysts.[230] A methanation rate equation of $r = kC_{CO_2}^{0.68}C_{H_2}^{3.31}$ was obtained with active energy of 73.1 kJ mol^{-1}.[230] Similarly, Kwak *et al.*[124] measured the carbon dioxide methanation reaction rates over Ru/Al_2O_3 and the estimated apparent activation energies was 62 kJ mol^{-1}. Carbon dioxide methanation kinetics was also used as a tool to reveal key insights into the role of platinum in promoted cobalt catalysis, H atom spillover and surface diffusion.[231–233] It is found that increasing the spatial separation between discrete cobalt and platinum entities results in a dramatic ~50% drop in apparent activation energy compared with that over pure cobalt ($E_a = 80$ kJ mol^{-1}) in carbon dioxide methanation.

However, the arguments about the carbon dioxide methanation with or without the formation of carbon monoxide intermediate still exist. Further investigations are needed to determine the difference of carbon dioxide activation on different active metal surfaces, which should be the key to understand the mechanism in carbon dioxide conversion reactions.

5. Other aspects of methanation process

Over the past years, researchers have developed some new processes for methanation reaction, among which sorption assisted methanation is one of the most important ones.[203,234,235] The sorption enhanced methanation reaction process showed unique performances for high grade SNG production at low methanation pressure. Photo-assisted catalytic methanation of carbon monoxide was also introduced over some semiconductor materials such as TiO_2.[236] Complete photocatalytic reduction of carbon dioxide to methane by hydrogen under solar light irradiation was also reported.[237] Ternary diagrams were applied in the design of methanation systems[238] and novel biochemical catalyzed methanation at mesophilic temperatures and ambient pressures have also been realized.[239,240] Moreover, methanation reactor and operation conditions were thoroughly investigated.[82,241–247] Fluidized bed reactor showed better performance than fixed bed in methanation process for SNG production in lab scale.[4,34,35,200,248–254] But so far, no fluidized bed reactor for SNG production has been reported in industrial scale yet. Several problems including attrition of catalysts, stability of fluidized state, and difficulty of scaling-up still require further investigations. Methanation of syngas in slurry-phase bubble-column reactors was also investigated because they have good heat-removal capabilities and the catalysts can be exchanged on-line.[155,255] The results show that the temperature of the catalyst bed is more stable and uniform in a slurry reactor as compared with that in a fixed bed reactor, therefore, using a slurry reactor is one potential route for syngas methanation. Magnetic fluidized bed,[111] dielectric barrier discharge plasma reactor,[256] micro-channel reactor[257] were also studied recently, which may inspire some new ideas for the methanation reactor development.

6. Conclusions and outlook

In conclusion, we have summarized the recent developments of carbon monoxide and carbon dioxide methanation catalysts for the production of SNG. Developing methanation catalysts with high activity at low temperature and high stability at high temperature are crucial for the methanation process because of the strong exothermic characteristic. How to increase the activity and stability of Ni catalysts and decrease/avoid the formation of $Ni(CO)_4$ at low temperature still need further investigation. High mechanical strength and hydrothermal stability are also essential to maintain long catalyst stability under industrial conditions. Carbon deposition could be alleviated by controlling the reaction conditions, which should not be the major problem. Decreasing the rate of active metal sintering under high temperature is another big challenge to increase the stability of methanation catalysts. Mo based catalysts show high potential for sulphur-resistant methanation catalysis but the activity needs to be further enhanced. Theoretical calculations should be combined with experiments to further explore the methanation reaction mechanisms and to improve the methanation catalyst design. Surface characterization at high pressure would bridge the gap between surface science and heterogeneous catalysis under real reaction conditions. New methanation reactors and processes shall advance the methanation progress together with the catalyst design.

Acknowledgements

The authors gratefully acknowledge the supports from the National Natural Science Foundation of China (no. 21476238), the National Basic Research Program (nos 2011CB200906 and 2014CB744306), and "Strategic Priority Research Program" of the Chinese Academy of Sciences (nos XDA07010100 and XDA07010200), and the National Research Foundation of Singapore (M4098015.121).

References

1 S. Ma, Y. Tan and Y. Han, *J. Nat. Gas Chem.*, 2011, **20**, 435–440.
2 I. Kiendl, M. Klemm, A. Clemens and A. Herrman, *Fuel*, 2014, **123**, 211–217.
3 R. Razzaq, C. S. Li and S. J. Zhang, *Fuel*, 2013, **113**, 287–299.
4 J. Kopyscinski, M. C. Seemann, R. Moergeli, S. M. A. Biollaz and T. J. Schildhauer, *Appl. Catal., A*, 2013, **462–463**, 150–156.
5 H. Arakawa, M. Aresta, J. N. Armor, M. A. Barteau, E. J. Beckman, A. T. Bell, J. E. Bercaw, C. Creutz, E. Dinjus, D. A. Dixon, K. Domen, D. L. DuBois, J. Eckert,

E. Fujita, D. H. Gibson, W. A. Goddard, D. W. Goodman, J. Keller, G. J. Kubas, H. H. Kung, J. E. Lyons, L. E. Manzer, T. J. Marks, K. Morokuma, K. M. Nicholas, R. Periana, L. Que, J. Rostrup-Nielson, W. M. H. Sachtler, L. D. Schmidt, A. Sen, G. A. Somorjai, P. C. Stair, B. R. Stults and W. Tumas, *Chem. Rev.*, 2001, **101**, 953–996.
6 C. Song, *Catal. Today*, 2006, **115**, 2–32.
7 E. V. Kondratenko, G. Mul, J. Baltrusaitis, G. O. Larrazábal and J. Pérez-Ramírez, *Energy Environ. Sci.*, 2013, **6**, 3112–3135.
8 K. Müller, M. Fleige, F. Rachow and D. Schmeißer, *Energy Procedia*, 2013, **40**, 240–248.
9 K. Müller, M. Städter, F. Rachow, D. Hoffmannbeck and D. Schmeißer, *Environ. Earth Sci.*, 2013, **70**, 3771–3778.
10 P. Sabatier and J. B. Senderens, *C. R. Acad. Sci.*, 1902, **134**, 514–516.
11 M. A. Vannice, *J. Catal.*, 1975, **37**, 449–461.
12 M. A. Vannice, *J. Catal.*, 1975, **37**, 462–473.
13 M. A. Vannice, *J. Catal.*, 1975, **40**, 129–134.
14 M. A. Vannice, *J. Catal.*, 1976, **44**, 152–162.
15 M. A. Vannice, *J. Catal.*, 1977, **50**, 228–236.
16 G. A. Mills and F. W. Steffgen, *Catal. Rev.: Sci. Eng.*, 1974, **8**, 159–210.
17 J. R. Rostrup Nielsen, K. Pedersen and J. Sehested, *Appl. Catal., A*, 2007, **330**, 134–138.
18 T. T. M. Nguyen, L. Wissing and M. S. Skjoth-Rasmussen, *Catal. Today*, 2013, **215**, 233–238.
19 J. Kopyscinski, T. J. Schildhauer and S. M. A. Biollaz, *Fuel*, 2010, **89**, 1763–1783.
20 W. Wang, S. Wang, X. Ma and J. Gong, *Chem. Soc. Rev.*, 2011, **40**, 3703–3727.
21 B. Wang, G. Ding, Y. Shang, J. Lv, H. Wang, E. Wang, Z. Li, X. Ma, S. Qin and Q. Sun, *Appl. Catal., A*, 2012, **431–432**, 144–150.
22 P. R. Wentrcek, B. J. Wood and H. Wise, *J. Catal.*, 1976, **43**, 363–366.
23 Y. Borodko and G. A. Somorjai, *Appl. Catal., A*, 1999, **186**, 355–362.
24 J. Gao, Y. Wang, Y. Ping, D. Hu, G. Xu, F. Gu and F. Su, *RSC Adv.*, 2012, **2**, 2358–2368.
25 S. I. Fujita and N. Takezawa, *Chem. Eng. J.*, 1997, **68**, 63–68.
26 T. Bligaard, J. K. Nørskov, S. Dahl, J. Matthiesen, C. H. Christensen and J. Sehested, *J. Catal.*, 2004, **224**, 206–217.
27 J. Nørskov, *J. Catal.*, 2002, **209**, 275–278.
28 G. Zhang, T. Sun, J. Peng, S. Wang and S. Wang, *Appl. Catal., A*, 2013, **462–463**, 75–81.
29 D. Hu, J. Gao, Y. Ping, L. Jia, P. Gunawan, Z. Zhong, G. Xu, F. Gu and F. Su, *Ind. Eng. Chem. Res.*, 2012, **51**, 4875–4886.
30 H. Qin, C. Guo, Y. Wu and J. Zhang, *Korean J. Chem. Eng.*, 2014, 1–6.
31 S. Hwang, J. Lee, U. G. Hong, J. G. Seo, J. C. Jung, D. J. Koh, H. Lim, C. Byun and I. K. Song, *J. Ind. Eng. Chem.*, 2011, **17**, 154–157.
32 J. Gao, C. Jia, J. Li, M. Zhang, F. Gu, G. Xu, Z. Zhong and F. Su, *Catal. Sci. Technol.*, 2013, **3**, 2009–2015.
33 J. Gao, C. Jia, J. Li, M. Zhang, F. Gu, G. Xu, Z. Zhong and F. Su, *J. Energy Chem.*, 2013, **22**, 919–927.
34 J. Li, L. Zhou, P. C. Li, Q. S. Zhu, J. J. Gao, F. N. Gu and F. B. Su, *Chem. Eng. J.*, 2013, **219**, 183–189.
35 J. Liu, W. Shen, D. Cui, J. Yu, F. Su and G. Xu, *Catal. Commun.*, 2013, **38**, 35–39.
36 V. M. Shinde and G. Madras, *AIChE J.*, 2014, **60**, 1027–1035.
37 X. Chen, J. Jin, G. Sha, C. Li, B. Zhang, D. Su, C. T. Williams and C. Liang, *Catal. Sci. Technol.*, 2014, **4**, 53–61.
38 J. Zhang, Z. Xin, X. Meng and M. Tao, *Fuel*, 2013, **109**, 693–701.
39 C. Jia, J. Gao, J. Li, F. Gu, G. Xu, Z. Zhong and F. Su, *Catal. Sci. Technol.*, 2013, **3**, 490–499.
40 J. Gao, C. Jia, M. Zhang, F. Gu, G. Xu, Z. Zhong and F. Su, *RSC Adv.*, 2013, **3**, 18156–18163.
41 J. Gao, C. Jia, J. Li, F. Gu, G. Xu, Z. Zhong and F. Su, *Ind. Eng. Chem. Res.*, 2012, **51**, 10345–10353.
42 J. Zhang, Z. Xin, X. Meng, Y. Lv and M. Tao, *Fuel*, 2014, **116**, 25–33.
43 H. Zhu, R. Razzaq, L. Jiang and C. Li, *Catal. Commun.*, 2012, **23**, 43–47.
44 H. Wang, Y. Fang, Y. Liu and X. Bai, *J. Nat. Gas Chem.*, 2012, **21**, 745–752.
45 Q. Pan, J. Peng, T. Sun, D. Gao, S. Wang and S. Wang, *Fuel Process. Technol.*, 2014, **123**, 166–171.
46 J. Liu, C. Li, F. Wang, S. He, H. Chen, Y. Zhao, M. Wei, D. G. Evans and X. Duan, *Catal. Sci. Technol.*, 2013, **3**, 2627–2633.
47 G. Zhou, T. Wu, H. Xie and X. Zheng, *Int. J. Hydrogen Energy*, 2013, **38**, 10012–10018.
48 T. Abe, M. Tanizawa, K. Watanabe and A. Taguchi, *Energy Environ. Sci.*, 2009, **2**, 315–321.
49 S. Tada, T. Shimizu, H. Kameyama, T. Haneda and R. Kikuchi, *Int. J. Hydrogen Energy*, 2012, **37**, 5527–5531.
50 Y. R. Li, G. X. Lu and J. T. Ma, *RSC Adv.*, 2014, **4**, 17420–17428.
51 M. A. A. Aziz, A. A. Jalil, S. Triwahyono, R. R. Mukti, Y. H. Taufiq-Yap and M. R. Sazegar, *Appl. Catal., B*, 2014, **147**, 359–368.
52 S. He, C. Li, H. Chen, D. Su, B. Zhang, X. Cao, B. Wang, M. Wei, D. G. Evans and X. Duan, *Chem. Mater.*, 2013, **25**, 1040–1046.
53 W. Zhen, B. Li, G. Lu and J. Ma, *RSC Adv.*, 2014, **4**, 16472–16479.
54 S. Tada, O. J. Ochieng, R. Kikuchi, T. Haneda and H. Kameyama, *Int. J. Hydrogen Energy*, 2014, **39**, 10090–10100.
55 S. Sharma, Z. Hu, P. Zhang, E. W. McFarland and H. Metiu, *J. Catal.*, 2011, **278**, 297–309.
56 G. Du, S. Lim, Y. Yang, C. Wang, L. Pfefferle and G. Haller, *J. Catal.*, 2007, **249**, 370–379.
57 S. Rahmani, M. Rezaei and F. Meshkani, *J. Ind. Eng. Chem.*, 2014, **20**, 1346–1352.
58 M. Guo and G. Lu, *React. Kinet., Mech. Catal.*, 2014, **113**, 101–113.
59 B. C. Enger and A. Holmen, *Catal. Rev.*, 2012, **54**, 437–488.

60 P. Riani, G. Garbarino, M. A. Lucchini, F. Canepa and G. Busca, *J. Mol. Catal. A: Chem.*, 2014, **383–384**, 10–16.
61 S. K. Ryi, S. W. Lee, K. R. Hwang and J. S. Park, *Fuel*, 2012, **94**, 64–69.
62 G. Lee, M. Moon, J. Park, S. Park and S. Hong, *Korean J. Chem. Eng.*, 2005, **22**, 541–546.
63 S. Hwang, J. Lee, U. G. Hong, J. H. Baik, D. J. Koh, H. Lim and I. K. Song, *J. Ind. Eng. Chem.*, 2013, **19**, 698–703.
64 Y.-Z. Wang, F.-M. Li, H.-M. Cheng, L.-Y. Fan and Y.-X. Zhao, *J. Fuel Chem. Technol.*, 2013, **41**, 972–977.
65 C. W. Hu, J. Yao, H. Q. Yang, Y. Chen and A. M. Tian, *J. Catal.*, 1997, **166**, 1–7.
66 P. Munnik, M. E. Velthoen, P. E. de Jongh, K. P. de Jong and C. J. Gommes, *Angew. Chem., Int. Ed.*, 2014, **126**, 9647–9651.
67 L. He, Q. Lin, Y. Liu and Y. Huang, *J. Energy Chem.*, 2014, **23**, 587–592.
68 N. Yao, H. Ma, Y. Shao, C. Yuan, D. Lv and X. Li, *J. Mater. Chem.*, 2011, **21**, 17403–17412.
69 B. Sen and M. A. Vannice, *J. Catal.*, 1991, **130**, 9–20.
70 C. Deleitenburg and A. Trovarelli, *J. Catal.*, 1995, **156**, 171–174.
71 M. A. Vannice, S. Y. Wang and S. H. Moon, *J. Catal.*, 1981, **71**, 152–166.
72 M. A. Vannice and R. L. Garten, *J. Catal.*, 1979, **56**, 236–248.
73 M. Jiang, B. Wang, Y. Yao, Z. Li, X. Ma, S. Qin and Q. Sun, *Appl. Surf. Sci.*, 2013, **285**(Part B), 267–277.
74 M. A. A. Aziz, A. A. Jalil, S. Triwahyono and S. M. Sidik, *Appl. Catal., A*, 2014, **486**, 115–122.
75 I. Czekaj, F. Loviat, F. Raimondi, J. Wambach, S. Biollaz and A. Wokaun, *Appl. Catal., A*, 2007, **329**, 68–78.
76 G. Garbarino, I. Valsamakis, P. Riani and G. Busca, *Catal. Commun.*, 2014, **51**, 37–41.
77 Z. Qin, J. Ren, M. Miao, Z. Li, J. Lin and K. Xie, *Appl. Catal., B*, 2015, **164**, 18–30.
78 M. P. Andersson, E. Abild Pedersen, I. N. Remediakis, T. Bligaard, G. Jones, J. Engbwk, O. Lytken, S. Horch, J. H. Nielsen, J. Sehested, J. R. Rostrup Nielsen, J. K. Norskov and I. Chorkendorff, *J. Catal.*, 2008, **255**, 6–19.
79 T. Shido, M. Lok and R. Prins, *Top. Catal.*, 1999, **8**, 223–236.
80 J. Sehested, *Catal. Today*, 2006, **111**, 103–110.
81 H. H. Gierlich, M. Fremery, A. Skov and J. R. Rostrup-Nielsen, Deactivation Phenomena of a Ni-based Catalyst for High Temperature Methanation, in *Studies in Surface Science and Catalysis*, ed. B. Delmon and G. F. Froment, Elsevier, 1980, pp. 459–469.
82 X. Bai, S. Wang, T. Sun and S. Wang, *Catal. Lett.*, 2014, 1–10.
83 C. H. Bartholomew, *Catal. Rev.: Sci. Eng.*, 1982, **24**, 67–112.
84 S. Helveg, C. Lopez-Cartes, J. Sehested, P. L. Hansen, B. S. Clausen, J. R. Rostrup-Nielsen, F. Abild-Pedersen and J. K. Norskov, *Nature*, 2004, **427**, 426–429.
85 T. Inui, T. Hagiwara and Y. Takegami, *Fuel*, 1982, **61**, 537–541.
86 E. Nikolla, A. Holewinski, J. Schwank and S. Linic, *J. Am. Chem. Soc.*, 2006, **128**, 11354–11355.
87 J. Lu, B. Fu, M. C. Kung, G. Xiao, J. W. Elam, H. H. Kung and P. C. Stair, *Science*, 2012, **335**, 1205–1208.
88 Q. Liu, J. Gao, M. Zhang, H. Li, F. Gu, G. Xu, Z. Zhong and F. Su, *RSC Adv.*, 2014, **4**, 16094–16103.
89 J. Sehested, A. Carlsson, T. V. W. Janssens, P. L. Hansen and A. K. Datyey, *J. Catal.*, 2001, **197**, 200–209.
90 J. Sehested, *J. Catal.*, 2003, **217**, 417–426.
91 J. Sehested, *J. Catal.*, 2004, **223**, 432–443.
92 J. Sehested, J. A. P. Gelten and S. Helveg, *Appl. Catal., A*, 2006, **309**, 237–246.
93 R. M. Ravenelle, J. R. Copeland, W.-G. Kim, J. C. Crittenden and C. Sievers, *ACS Catal.*, 2011, **1**, 552–561.
94 X. Bai, S. Wang, T. Sun and S. Wang, *React. Kinet., Mech. Catal.*, 2014, **112**, 437–451.
95 A. M. Zhao, W. Y. Ying, H. T. Zhang, H. F. Ma and D. Y. Fang, *J. Nat. Gas Chem.*, 2012, **21**, 170–177.
96 A. M. Zhao, W. Y. Ying, H. T. Zhang, H. F. Ma and D. Y. Fang, *Catal. Commun.*, 2012, **17**, 34–38.
97 V. M. Gonzalez-Delacruz, R. Pereñiguez, F. Ternero, J. P. Holgado and A. Caballero, *ACS Catal.*, 2011, **1**, 82–88.
98 C. H. Bartholomew, G. D. Weatherbee and G. A. Jarvi, *J. Catal.*, 1979, **60**, 257–269.
99 B. Legras, V. V. Ordomsky, C. Dujardin, M. Virginie and A. Y. Khodakov, *ACS Catal.*, 2014, **4**, 2785–2791.
100 R. P. W. J. Struis, T. J. Schildhauer, I. Czekaj, M. Janousch, S. M. A. Biollaz and C. Ludwig, *Appl. Catal., A*, 2009, **362**, 121–128.
101 L. Jurgensen, E. A. Ehimen, J. Born, J. B. Holm-Nielsen and D. Rooney, *Bioresour. Technol.*, 2015, **178**, 319–322.
102 C. H. Bartholomew, *Appl. Catal., A*, 2001, **212**, 17–60.
103 C. Yuan, N. Yao, X. Wang, J. Wang, D. Lv and X. Li, *Chem. Eng. J.*, 2015, **260**, 1–10.
104 X. Yan, Y. Liu, B. Zhao, Y. Wang and C.-J. Liu, *Phys. Chem. Chem. Phys.*, 2013, **15**, 12132–12138.
105 G. Prieto, A. Martínez, P. Concepción and R. Moreno-Tost, *J. Catal.*, 2009, **266**, 129–144.
106 P. Concepcion, C. Lopez, A. Martinez and V. Puntes, *J. Catal.*, 2004, **228**, 321–332.
107 S. Rojanapipatkul and B. Jongsomjit, *Catal. Commun.*, 2008, **10**, 232–236.
108 B. Wang, Y. Yao, M. Jiang, Z. Li, X. Ma, S. Qin and Q. Sun, *J. Energy Chem.*, 2014, **23**, 35–42.
109 H. Zhu, R. Razzaq, C. Li, Y. Muhmmad and S. Zhang, *AIChE J.*, 2013, **59**, 2567–2576.
110 S. Hwang, J. Lee, U. G. Hong, J. C. Jung, D. J. Koh, H. Lim, C. Byun and I. K. Song, *J. Ind. Eng. Chem.*, 2012, **18**, 243–248.
111 J. Li, L. Zhou, Q. Zhu and H. Li, *Ind. Eng. Chem. Res.*, 2013, **52**, 6647–6654.
112 R. Razzaq, H. Zhu, L. Jiang, U. Muhammad, C. Li and S. Zhang, *Ind. Eng. Chem. Res.*, 2013, **52**, 2247–2256.
113 S. Alayoglu, S. K. Beaumont, F. Zheng, V. V. Pushkarev, H. Zheng, V. Iablokov, Z. Liu, J. Guo, N. Kruse and G. A. Somorjai, *Top. Catal.*, 2011, **54**, 778–785.
114 A. Tuxen, S. Carenco, M. Chintapalli, C. H. Chuang, C. Escudero, E. Pach, P. Jiang, F. Borondics, B. Beberwyck, A. P. Alivisatos, G. Thornton, W. F. Pong, J. H. Guo, R. Perez, F. Besenbacher and M. Salmeron, *J. Am. Chem. Soc.*, 2013, **135**, 2273–2278.

115 J.-X. Liu, H.-Y. Su and W.-X. Li, *Catal. Today*, 2013, **215**, 36–42.
116 D. Tian, Z. Liu, D. Li, H. Shi, W. Pan and Y. Cheng, *Fuel*, 2013, **104**, 224–229.
117 S. Hwang, U. G. Hong, J. Lee, J. G. Seo, J. H. Baik, D. J. Koh, H. Lim and I. K. Song, *J. Ind. Eng. Chem.*, 2013, **19**, 2016–2021.
118 M. P. Andersson, T. Bligaard, A. Kustov, K. E. Larsen, J. Greeley, T. Johannessen, C. H. Christensen and J. K. Norskov, *J. Catal.*, 2006, **239**, 501–506.
119 S. Hwang, U. Hong, J. Lee, J. Baik, D. Koh, H. Lim and I. Song, *Catal. Lett.*, 2012, **142**, 860–868.
120 S. Eckle, Y. Denkwitz and R. J. Behm, *J. Catal.*, 2010, **269**, 255–268.
121 C. Janke, M. S. Duyar, M. Hoskins and R. Farrauto, *Appl. Catal., B*, 2014, **152–153**, 184–191.
122 F. Masini, C. E. Strebel, D. N. McCarthy, A. U. F. Nierhoff, J. Kehres, E. M. Fiordaliso, J. H. Nielsen and I. Chorkendorff, *J. Catal.*, 2013, **308**, 282–290.
123 B. T. Loveless, C. Buda, M. Neurock and E. Iglesia, *J. Am. Chem. Soc.*, 2013, **135**, 6107–6121.
124 J. H. Kwak, L. Kovarik and J. Szanyi, *ACS Catal.*, 2013, **3**, 2449–2455.
125 C. F. J. König, T. J. Schildhauer and M. Nachtegaal, *J. Catal.*, 2013, **305**, 92–100.
126 W. J. Shen, M. Okumura, Y. Matsumura and M. Haruta, *Appl. Catal., A*, 2001, **213**, 225–232.
127 S. Y. Wang, S. H. Moon and M. A. Vannice, *J. Catal.*, 1981, **71**, 167–174.
128 J. Martins, N. Batail, S. Silva, S. Rafik-Clement, A. Karelovic, D. P. Debecker, A. Chaumonnot and D. Uzio, *Catal. Commun.*, 2015, **58**, 11–15.
129 H. Yoshida, K. Watanabe, N. Iwasa, S.-I. Fujita and M. Arai, *Appl. Catal., B*, 2015, **162**, 93–97.
130 M. A. Vannice and C. C. Twu, *J. Catal.*, 1983, **82**, 213–222.
131 K.-P. Yu, W.-Y. Yu, M.-C. Kuo, Y.-C. Liou and S.-H. Chien, *Appl. Catal., B*, 2008, **84**, 112–118.
132 C. Swalus, M. Jacquemin, C. Poleunis, P. Bertrand and P. Ruiz, *Appl. Catal., B*, 2012, **125**, 41–50.
133 A. Karelovic and P. Ruiz, *Appl. Catal., B*, 2012, **113–114**, 237–249.
134 A. Trovarelli, C. Deleitenburg, G. Dolcetti and J. L. Lorca, *J. Catal.*, 1995, **151**, 111–124.
135 S. Zaman and K. J. Smith, *Catal. Rev.*, 2012, **54**, 41–132.
136 M. Y. Kim, S. B. Ha, D. J. Koh, C. Byun and E. D. Park, *Catal. Commun.*, 2013, **35**, 68–71.
137 L. Y. Novoselova, *J. Alloys Compd.*, 2014, **615**, 784–791.
138 J. Liu, E. Wang, J. Lv, Z. Li, B. Wang, X. Ma, S. Qin and Q. Sun, *Fuel Process. Technol.*, 2013, **110**, 249–257.
139 A. E. Aksoylu, Z. Mısırlı and Z. . İ. Önsan, *Appl. Catal., A*, 1998, **168**, 385–397.
140 B. Wang, Y. Shang, G. Ding, J. Lv, H. Wang, E. Wang, Z. Li, X. Ma, S. Qin and Q. Sun, *React. Kinet., Mech. Catal.*, 2012, **106**, 495–506.
141 M. Jiang, B. Wang, Y. Yao, H. Wang, Z. Li, X. Ma, S. Qin and Q. Sun, *Catal. Commun.*, 2013, **35**, 32–35.
142 M. Jiang, B. Wang, Y. Yao, H. Wang, Z. Li, X. Ma, S. Qin and Q. Sun, *Appl. Catal., A*, 2014, **469**, 89–97.
143 M. Jiang, B. Wang, J. Lv, H. Wang, Z. Li, X. Ma, S. Qin and Q. Sun, *Appl. Catal., A*, 2013, **466**, 224–232.
144 M. Jiang, B. Wang, Y. Yao, Z. Li, X. Ma, S. Qin and Q. Sun, *Catal. Sci. Technol.*, 2013, **3**, 2793–2800.
145 Z. Li, H. Wang, E. Wang, J. Lv, Y. Shang, G. Ding, B. Wang, X. Ma, S. Qin and Q. Su, *Kinet. Catal.*, 2013, **54**, 338–343.
146 I. Levin and D. Brandon, *J. Am. Ceram. Soc.*, 1998, **81**, 1995–2012.
147 G. Garbarino, P. Riani, L. Magistri and G. Busca, *Int. J. Hydrogen Energy*, 2014, **39**, 11557–11565.
148 A. Tougerti, I. Llorens, F. D'Acapito, E. Fonda, J. L. Hazemann, Y. Joly, D. Thiaudiere, M. Che and X. Carrier, *Angew. Chem., Int. Ed.*, 2012, **51**, 7697–7701.
149 X. Zhang, W.-j. Sun and W. Chu, *J. Fuel Chem. Technol.*, 2013, **41**, 96–101.
150 X. L. Yan, Y. Liu, B. R. Zhao, Z. Wang, Y. Wang and C. J. Liu, *Int. J. Hydrogen Energy*, 2013, **38**, 2283–2291.
151 M. A. A. Aziz, A. A. Jalil, S. Triwahyono and M. W. A. Saad, *Chem. Eng. J.*, 2015, **260**, 757–764.
152 S.-D. Mo and W. Ching, *Phys. Rev. B: Condens. Matter Mater. Phys.*, 1995, **51**, 13023–13032.
153 Y. Zeng, H. Ma, H. Zhang, W. Ying and D. Fang, *Fuel*, 2014, **137**, 155–163.
154 J. Barrientos, M. Lualdi, M. Boutonnet and S. Järås, *Appl. Catal., A*, 2014, **486**, 143–149.
155 J. Zhang, Y. Bai, Q. Zhang, X. Wang, T. Zhang, Y. Tan and Y. Han, *Fuel*, 2014, **132**, 211–218.
156 Z. Li, Y. Tian, J. He, B. Wang and X. Ma, *J. Energy Chem.*, 2014, **23**, 625–632.
157 Y.-H. Huang, J.-J. Wang, Z.-M. Liu, G.-D. Lin and H.-B. Zhang, *Appl. Catal., A*, 2013, **466**, 300–306.
158 A. Chen, T. Miyao, K. Higashiyama and M. Watanabe, *Catal. Sci. Technol.*, 2014, **4**, 2508–2511.
159 N. Perkas, G. Amirian, Z. Y. Zhong, J. Teo, Y. Gofer and A. Gedanken, *Catal. Lett.*, 2009, **130**, 455–462.
160 W. Q. Xu, Z. Y. Liu, A. C. Johnston-Peck, S. D. Senanayake, G. Zhou, D. Stacchiola, E. A. Stach and J. A. Rodriguez, *ACS Catal.*, 2013, **3**, 975–984.
161 I. I. Soykal, H. Sohn, D. Singh, J. T. Miller and U. S. Ozkan, *ACS Catal.*, 2014, **4**, 585–592.
162 A. Trovarelli, *Catal. Rev.: Sci. Eng.*, 1996, **38**, 439–520.
163 M. M. Zyryanova, P. V. Snytnikov, R. V. Gulyaev, Y. I. Amosov, A. I. Boronin and V. A. Sobyanin, *Chem. Eng. J.*, 2014, **238**, 189–197.
164 G. Vilé, S. Colussi, F. Krumeich, A. Trovarelli and J. Pérez-Ramírez, *Angew. Chem.*, 2014, **126**, 12265–12268.
165 S. D. Senanayake, J. Evans, S. Agnoli, L. Barrio, T.-L. Chen, J. Hrbek and J. A. Rodriguez, *Top. Catal.*, 2011, **54**, 34–41.
166 R. Razzaq, C. Li, N. Amin, S. Zhang and K. Suzuki, *Energy Fuels*, 2013, **27**, 6955–6961.
167 W. Cai, Q. Zhong and Y. Zhao, *Catal. Commun.*, 2013, **39**, 30–34.
168 Z. Wang, Q. Fu and X. Bao, *Progr. Chem.*, 2014, **26**, 502–511.
169 M. Ledoux and C. Pham-Huu, *CATTECH*, 2001, **5**, 226–246.

170 G. Zhang, J. Peng, T. Sun and S. Wang, *Chin. J. Catal.*, 2013, **34**, 1745–1755.
171 Y. Yu, G. Q. Jin, Y. Y. Wang and X. Y. Guo, *Fuel Process. Technol.*, 2011, **92**, 2293–2298.
172 Y. Yu, G. Jin, Y. Wang and X. Guo, *Catal. Commun.*, 2013, **31**, 5–10.
173 M. A. Vannice, Y. L. Chao and R. M. Friedman, *Appl. Catal.*, 1986, **20**, 91–107.
174 L. Song, Y. Yu, X. Wang, G. Jin, Y. Wang and X. Y. Guo, *Korean Chem. Eng. Res.*, 2014, **52**, 678–687.
175 J. Zhu, H. Li, L. Zhong, P. Xiao, X. Xu, X. Yang, Z. Zhao and J. Li, *ACS Catal.*, 2014, **4**, 2917–2940.
176 M. A. Pena and J. L. G. Fierro, *Chem. Rev.*, 2001, **101**, 1981–2017.
177 F. W. Chang, T. J. Hsiao, S. W. Chung and J. J. Lo, *Appl. Catal., A*, 1997, **164**, 225–236.
178 F. W. Chang, T. J. Hsiao and J. D. Shih, *Ind. Eng. Chem. Res.*, 1998, **37**, 3838–3845.
179 F.-W. Chang, M.-S. Kuo, M.-T. Tsay and M.-C. Hsieh, *Appl. Catal., A*, 2003, **247**, 309–320.
180 H. Lu, X. Yang, G. Gao, K. Wang, Q. Shi, J. Wang, C. Han, J. Liu, M. Tong, X. Liang and C. Li, *Int. J. Hydrogen Energy*, 2014, **39**, 18894–18907.
181 M. F. Variava, T. L. Church, N. Noorbehesht, A. T. Harris and A. I. Minett, *Catal. Sci. Technol.*, 2015, **5**, 515–524.
182 J. Liu, J. Yu, F. Su and G. Xu, *Catal. Sci. Technol.*, 2014, **4**, 472–481.
183 M. Guo and G. Lu, *Catal. Commun.*, 2014, **54**, 55–60.
184 M. T. Fan, K. P. Miao, J. D. Lin, H. B. Zhang and D. W. Liao, *Appl. Surf. Sci.*, 2014, **307**, 682–688.
185 H. Y. Kim, H. M. Lee and J.-N. Park, *J. Phys. Chem. C*, 2010, **114**, 7128–7131.
186 Z. Li, L. Bian, Q. Zhu and W. Wang, *Kinet. Catal.*, 2014, **55**, 217–223.
187 H. G. J. L. Rotgerink, R. P. A. M. Paalman, J. G. van Ommen and J. R. H. Ross, *Appl. Catal.*, 1988, **45**, 257–280.
188 A. Zhao, W. Ying, H. Zhang, H. Ma and D. Fang, *Proc. World Acad. Sci. Eng. Tech.*, 2011, **59**, 1002–1006.
189 S. Tada, R. Kikuchi, A. Takagaki, T. Sugawara, S. Ted Oyama and S. Satokawa, *Catal. Today*, 2014, **232**, 16–21.
190 H. Liu, X. Zou, X. Wang, X. Lu and W. Ding, *J. Nat. Gas Chem.*, 2012, **21**, 703–707.
191 H. G. J. Lansink Rotgerink, J. C. Slaa, J. G. van Ommen and J. R. H. Ross, *Appl. Catal.*, 1988, **45**, 281–290.
192 H. G. J. L. Rotgerink, P. D. L. Mercera, J. G. van Ommen and J. R. H. Ross, *Appl. Catal.*, 1988, **45**, 239–256.
193 C. Guo, Y. Wu, H. Qin and J. Zhang, *Fuel Process. Technol.*, 2014, **124**, 61–69.
194 Q. Liu, F. Gu, X. Lu, Y. Liu, H. Li, Z. Zhong, G. Xu and F. Su, *Appl. Catal., A*, 2014, **488**, 37–47.
195 Y. Zeng, H. Ma, H. Zhang and W. Ying, *International Journal of Chemical, Nuclear, Metallurgical and Materials Engineering*, 2014, **8**, 582–586.
196 J. A. Schwarz, C. Contescu and A. Contescu, *Chem. Rev.*, 1995, **95**, 477–510.
197 E. C. Kruissink, E. B. M. Doesburg, L. L. van Reijen, L. E. Alzamora, S. Orr, J. R. H. Ross and G. van Veen, The Preparation and Pretreatment of Coprecipitated Nickel-Alumina Catalysts for Methanation at High Temperatures, in *Studies in Surface Science and Catalysis*, ed. P. G. P. J. B. Delmon and G. Poncelet, Elsevier, 1979, pp. 143–157.
198 X. Yang, X. Wang, G. Gao, Wendurima, E. Liu, Q. Shi, J. Zhang, C. Han, J. Wang, H. Lu, J. Liu and M. Tong, *Int. J. Hydrogen Energy*, 2013, **38**, 13926–13937.
199 X. Yang, Wendurima, G. Gao, Q. Shi, X. Wang, J. Zhang, C. Han, J. Wang, H. Lu, J. Liu and M. Tong, *Int. J. Hydrogen Energy*, 2014, **39**, 3231–3242.
200 B. Liu and S. Ji, *J. Energy Chem.*, 2013, **22**, 740–746.
201 S. Hwang, J. Lee, U. G. Hong, J. C. Jung, J. H. Baik, D. J. Koh, H. Lim and I. K. Song, *J. Nanosci. Nanotechnol.*, 2012, **12**, 6051–6057.
202 J. Zhang, Z. Xin, X. Meng, Y. Lv and M. Tao, *Ind. Eng. Chem. Res.*, 2013, **52**, 14533–14544.
203 A. Borgschulte, N. Gallandat, B. Probst, R. Suter, E. Callini, D. Ferri, Y. Arroyo, R. Erni, H. Geerlings and A. Zuttel, *Phys. Chem. Chem. Phys.*, 2013, **15**, 9620–9625.
204 A. Karelovic and P. Ruiz, *ACS Catal.*, 2013, **3**, 2799–2812.
205 L. E. Alzamora, J. R. H. Ross, E. C. Kruissink and L. L. Vanreijen, *J. Chem. Soc., Faraday Trans. 1*, 1981, **77**, 665–681.
206 E. C. Kruissink, L. L. Vanreijen and J. R. H. Ross, *J. Chem. Soc., Faraday Trans. 1*, 1981, **77**, 649–663.
207 M. G. O'Brien, S. D. M. Jacques, M. Di Michiel, P. Barnes, B. M. Weckhuysen and A. M. Beale, *Chem. Sci.*, 2012, **3**, 509–523.
208 B. Vos, E. Poels and A. Bliek, *J. Catal.*, 2001, **198**, 77–88.
209 G. P. Van Der Laan and A. A. C. M. Beenackers, *Catal. Rev.*, 1999, **41**, 255–318.
210 T. H. Pham, X. Z. Duan, G. Qian, X. G. Zhou and D. Chen, *J. Phys. Chem. C*, 2014, **118**, 10170–10176.
211 M. R. Elahifard, M. P. Jigato and J. W. Niemantsverdriet, *ChemPhysChem*, 2012, **13**, 89–91.
212 S. Shetty, A. P. J. Jansen and R. A. van Santen, *J. Am. Chem. Soc.*, 2009, **131**, 12874–12875.
213 M. Ojeda, R. Nabar, A. U. Nilekar, A. Ishikawa, M. Mavrikakis and E. Iglesia, *J. Catal.*, 2010, **272**, 287–297.
214 S. Eckle, H.-G. Anfang and R. J. r. Behm, *J. Phys. Chem. C*, 2011, **115**, 1361–1367.
215 P. Panagiotopoulou, D. I. Kondarides and X. E. Verykios, *J. Phys. Chem. C*, 2011, **115**, 1220–1230.
216 I. Alstrup, *J. Catal.*, 1995, **151**, 216–225.
217 D. W. Goodman, R. D. Kelley, T. E. Madey and J. T. Yates, *J. Catal.*, 1980, **63**, 226–234.
218 R. S. Polizzotti and J. A. Schwarz, *J. Catal.*, 1982, **77**, 1–15.
219 J. Sehested, S. Dahl, J. Jacobsen and J. R. Rostrup-Nielsen, *J. Phys. Chem. B*, 2004, **109**, 2432–2438.
220 J. Kopyscinski, T. J. Schildhauer, F. Vogel, S. M. A. Biollaz and A. Wokaun, *J. Catal.*, 2010, **271**, 262–279.
221 J. Zhang, N. Fatah, S. Capela, Y. Kara, O. Guerrini and A. Y. Khodakov, *Fuel*, 2013, **111**, 845–854.
222 A. C. Lausche, A. J. Medford, T. S. Khan, Y. Xu, T. Bligaard, F. Abild-Pedersen, J. K. Nørskov and F. Studt, *J. Catal.*, 2013, **307**, 275–282.

223 A. Karelovic and P. Ruiz, *J. Catal.*, 2013, **301**, 141–153.
224 S. Akamaru, T. Shimazaki, M. Kubo and T. Abe, *Appl. Catal., A*, 2014, **470**, 405–411.
225 P. A. U. Aldana, F. Ocampo, K. Kobl, B. Louis, F. Thibault-Starzyk, M. Daturi, P. Bazin, S. Thomas and A. C. Roger, *Catal. Today*, 2013, **215**, 201–207.
226 Q. Pan, J. Peng, T. Sun, S. Wang and S. Wang, *Catal. Commun.*, 2014, **45**, 74–78.
227 Q. S. Pan, J. X. Peng, S. Wang and S. D. Wang, *Catal. Sci. Technol.*, 2014, **4**, 502–509.
228 J.-N. Park and E. W. McFarland, *J. Catal.*, 2009, **266**, 92–97.
229 M. Marwood, R. Doepper and A. Renken, *Appl. Catal., A*, 1997, **151**, 223–246.
230 B. W. Lu and K. Kawamoto, *Catal. Sci. Technol.*, 2014, **4**, 4313–4321.
231 S. K. Beaumont, S. Alayoglu, C. Specht, N. Kruse and G. A. Somorjai, *Nano Lett.*, 2014, **14**, 4792–4796.
232 S. K. Beaumont, S. Alayoglu, C. Specht, W. D. Michalak, V. V. Pushkarev, J. Guo, N. Kruse and G. A. Somorjai, *J. Am. Chem. Soc.*, 2014, **136**, 9898–9901.
233 Z. A. Ibraeva, N. V. Nekrasov, B. S. Gudkov, V. I. Yakerson, Z. T. Beisembaeva, E. Z. Golosman and S. L. Kiperman, *Theor. Exp. Chem.*, 1991, **26**, 584–588.
234 S. Walspurger, G. D. Elzinga, J. W. Dijkstra, M. Sarić and W. G. Haije, *Chem. Eng. J.*, 2014, **242**, 379–386.
235 V. M. Lebarbier, R. A. Dagle, L. Kovarik, K. O. Albrecht, X. Li, L. Li, C. E. Taylor, X. Bao and Y. Wang, *Appl. Catal., B*, 2014, **144**, 223–232.
236 X. Lin, K. Yang, R. Si, X. Chen, W. Dai and X. Fu, *Appl. Catal., B*, 2014, **147**, 585–591.
237 F. Sastre, A. V. Puga, L. Liu, A. Corma and H. Garcia, *J. Am. Chem. Soc.*, 2014, **136**, 6798–6801.
238 V. Frick, J. Brellochs and M. Specht, *Fuel Process. Technol.*, 2014, **118**, 156–160.
239 M. Burkhardt and G. Busch, *Appl. Energy*, 2013, **111**, 74–79.
240 M. Burkhardt, T. Koschack and G. Busch, *Bioresour. Technol.*, 2015, **178**, 330–333.
241 W. Kang and K. Lee, *Korean J. Chem. Eng.*, 2013, **30**, 1386–1394.
242 R. Güttel, *Chem. Eng. Technol.*, 2013, **36**, 1675–1682.
243 H. Er-rbib and C. Bouallou, *C. R. Chim.*, 2014, **17**, 701–706.
244 N. R. Parlikkad, S. Chambrey, P. Fongarland, N. Fatah, A. Khodakov, S. Capela and O. Guerrini, *Fuel*, 2013, **107**, 254–260.
245 L.-J. Zhao and Q. Sun, *Int. J. Low-Carbon Technol.*, 2014, 1–6.
246 X. Li, B. Yang and Y. Zhang, *J. Process Control*, 2013, **23**, 1360–1370.
247 Y.-L. Kao, P.-H. Lee, Y.-T. Tseng, I. L. Chien and J. D. Ward, *J. Taiwan Inst. Chem. Eng.*, 2014, **45**, 2346–2357.
248 J. Liu, D. Cui, J. Yu, F. Su and G. Xu, *Chin. J. Chem. Eng.*, 2015, **23**, 86–92.
249 Y. Liu and O. Hinrichsen, *Ind. Eng. Chem. Res.*, 2014, **53**, 9348–9356.
250 M. C. Seemann, T. J. Schildhauer and S. M. A. Biollaz, *Ind. Eng. Chem. Res.*, 2010, **49**, 7034–7038.
251 J. Kopyscinski, T. J. Schildhauer and S. M. A. Biollaz, *Chem. Eng. Sci.*, 2011, **66**, 924–934.
252 J. Kopyscinski, T. J. Schildhauer and S. M. A. Biollaz, *Chem. Eng. Sci.*, 2011, **66**, 1612–1621.
253 J. Kopyscinski, T. J. Schildhauer and S. M. A. Biollaz, *Ind. Eng. Chem. Res.*, 2011, **50**, 2781–2790.
254 M. C. Seemann, T. J. Schildhauer and S. M. A. Biollaz, *Ind. Eng. Chem. Res.*, 2010, **49**, 7034–7038.
255 J. Lefebvre, M. Götz, S. Bajohr, R. Reimert and T. Kolb, *Fuel Process. Technol.*, 2015, **132**, 83–90.
256 E. Jwa, S. B. Lee, H. W. Lee and Y. S. Mok, *Fuel Process. Technol.*, 2013, **108**, 89–93.
257 Z. H. Liu, B. Z. Chu, X. L. Zhai, Y. Jin and Y. Cheng, *Fuel*, 2012, **95**, 599–605.